SAND2018-11754C

Synthesis of nanostructured ferroic materials for energy conversion

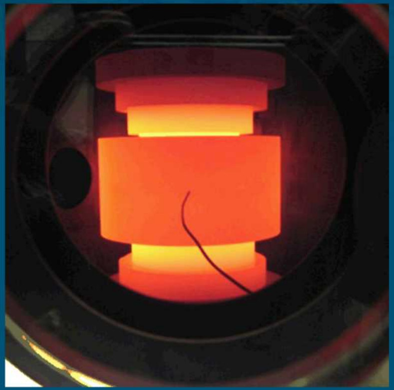

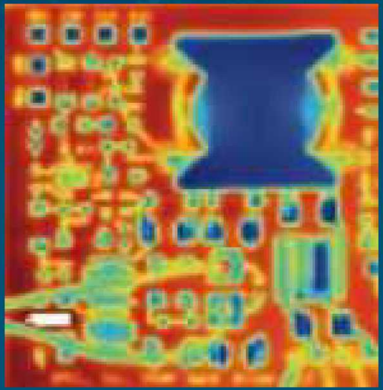

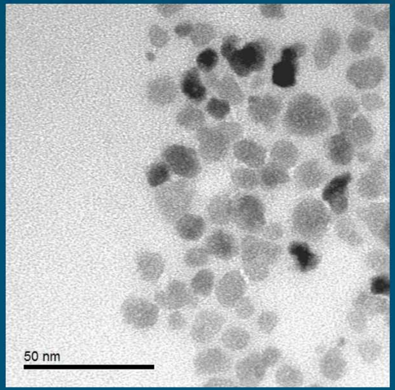

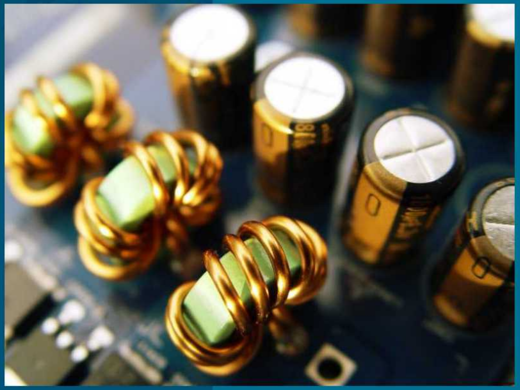

Todd C. Monson, Tyler E. Stevens, David A. Vargas
Sandia National Labs, tmonson@sandia.gov

Renee M. Van Ginhoven
Air Force Research Laboratory

Baolong Zheng, Yizhang Zhou, Martin Fraga, Enrique Lavernia
University of California, Irvine

Sandia National Laboratories is a multimission laboratory managed and operated by National Technology and Engineering Solutions of Sandia LLC, a wholly owned subsidiary of Honeywell International Inc. for the U.S. Department of Energy's National Nuclear Security Administration under contract DE-NA0003525.

Ferroics Impact Power Conversion Volume and Weight

Passive elements and thermal management comprise the bulk of the volume and mass of a power converter

WBG/UWBG materials enable higher switching frequency and better thermal management

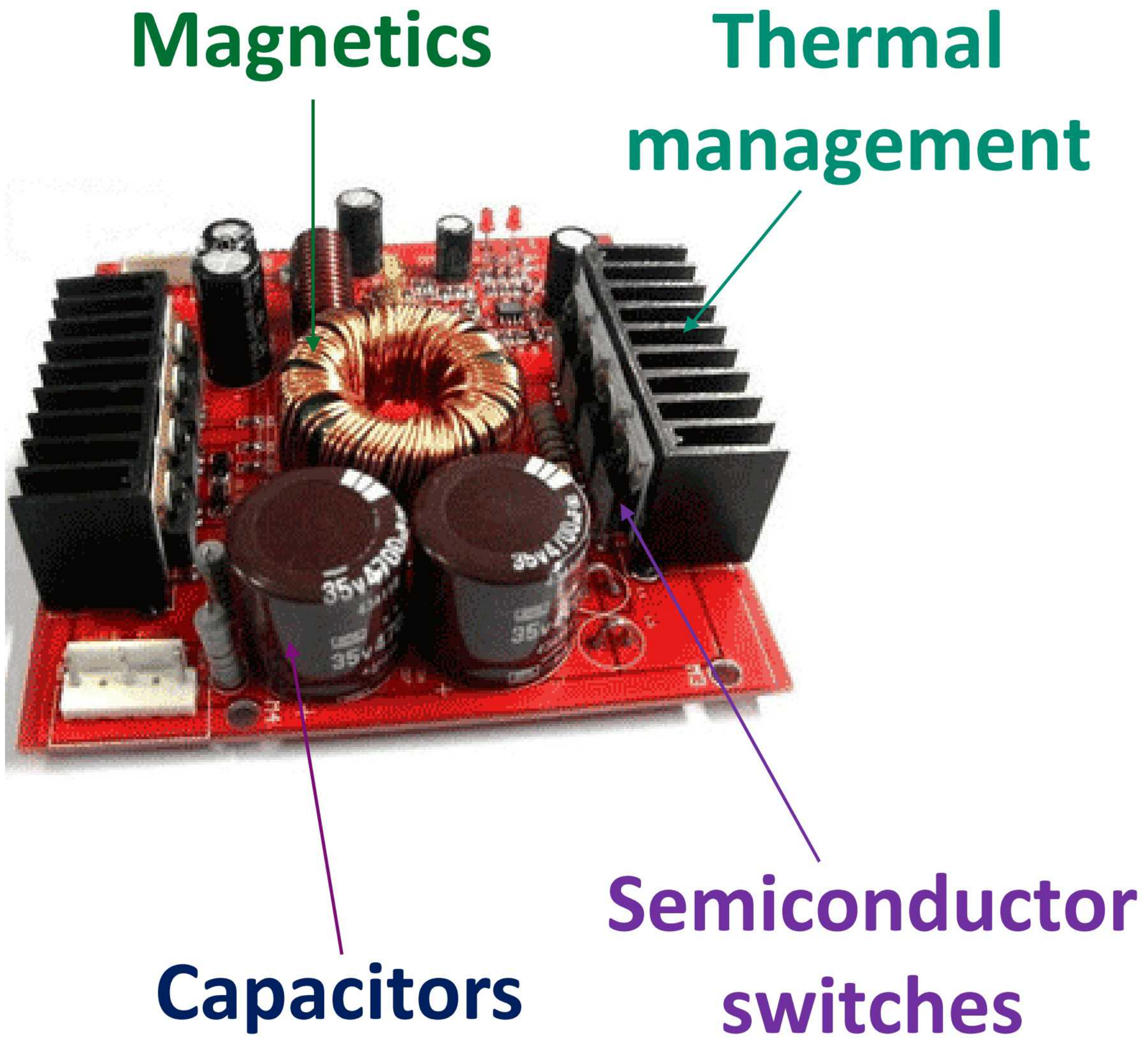

J. Neely, J. Flicker, B. Kaplar (SNL)

Ferroics

Size	Ferromagnetic	Ferroelectric	Ferroelastic
≈1µm-10^3 nm	Multidomain 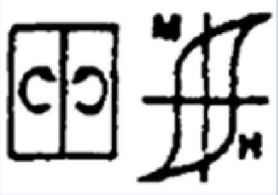	Multidomain 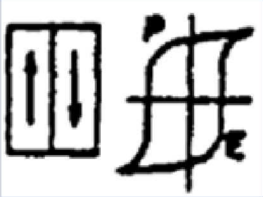	Multidomain 
≈0.1µm-10^2 nm	Single Domain 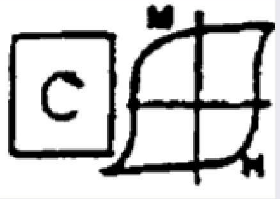	Single Domain 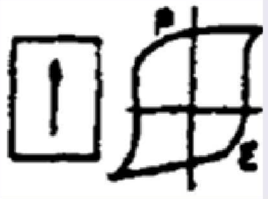	Single Domain 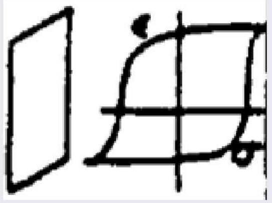
≈10nm-10^3 Å	Super-paramagnetic 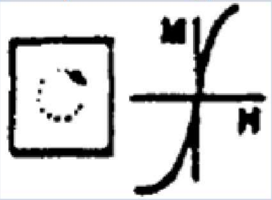	Super-Paraelectric 	Super-Paraelastic 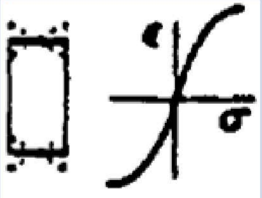
≈1nm-10 Å	Paramagnetic 	Paraelectric 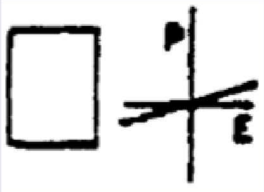	Paraelastic 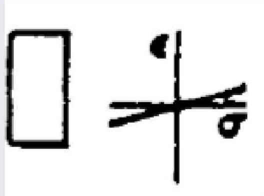

Newnham, R.E. "Size Effects in Ferroics", *Integrated Ferroelectrics*, 1998, Vol.20, pp. 1-13

Soft Magnetics (Iron Nitride)

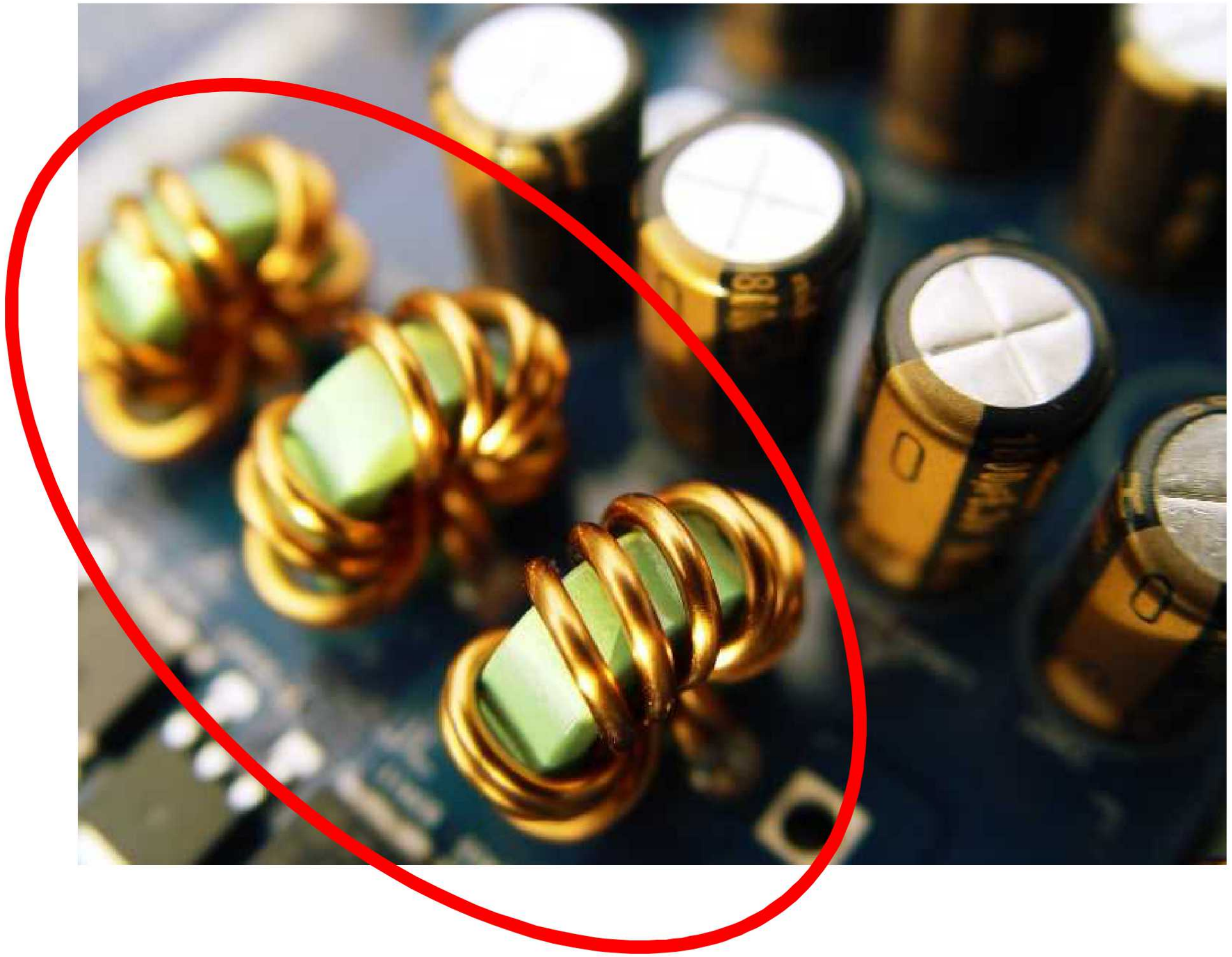

Hard vs. Soft Magnets

Hard (permanent) magnet

H_c > 1000 A/m

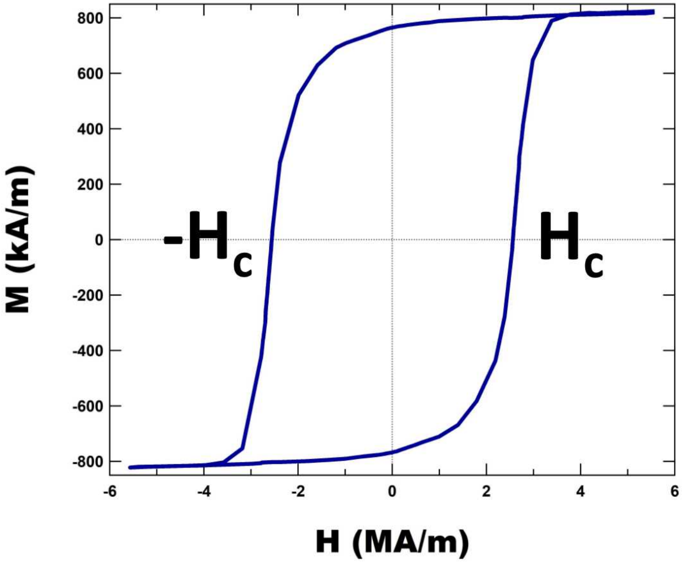

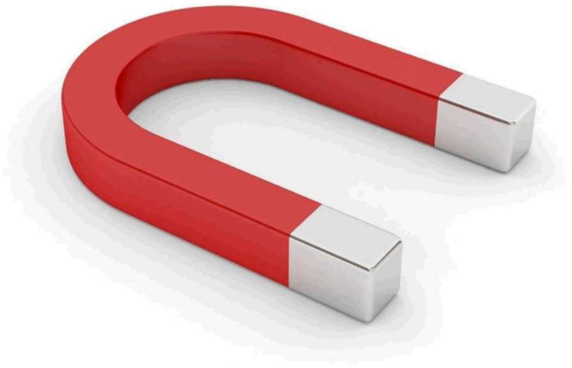

Soft magnet

H_c < 1000 A/m

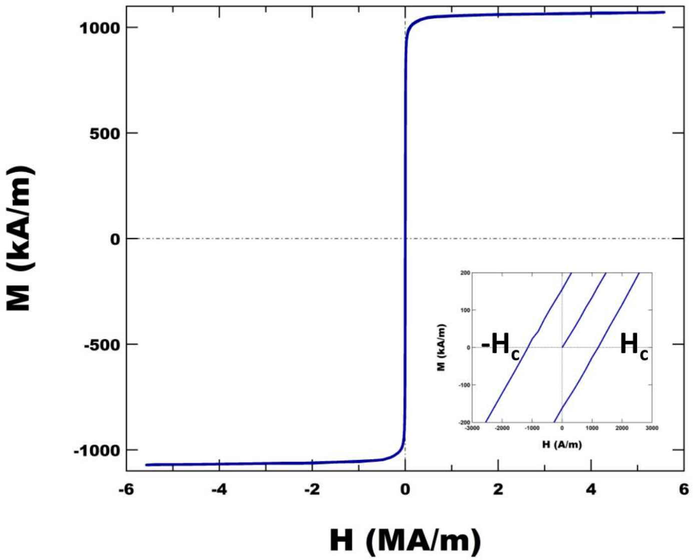

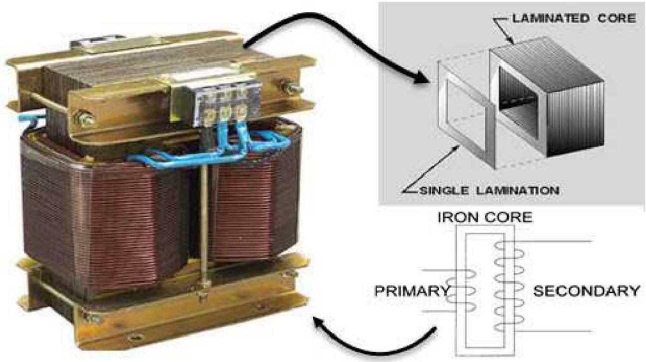

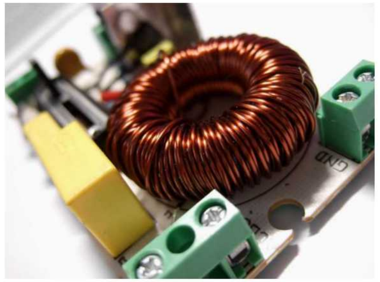

Soft Magnet Energy Related Applications

Inductor cores

Transformer cores

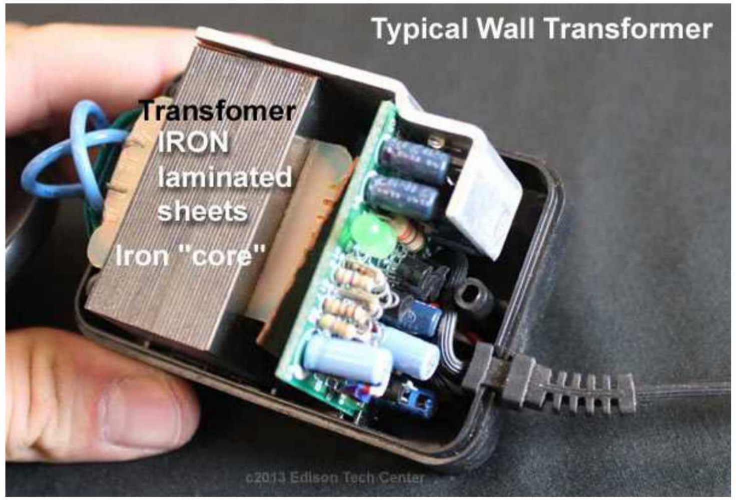

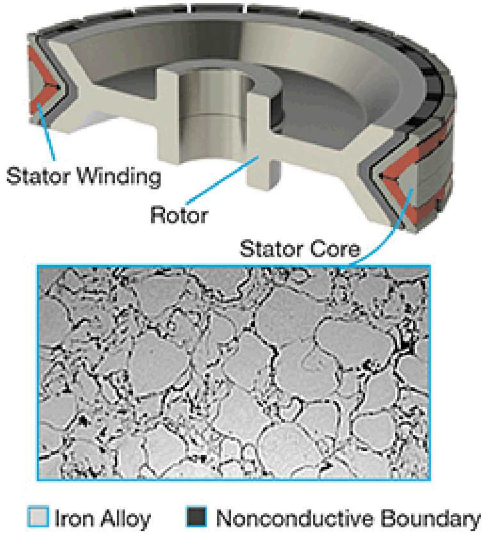

Electrical machines (motors & generators)

Soft Magnetic Material Development

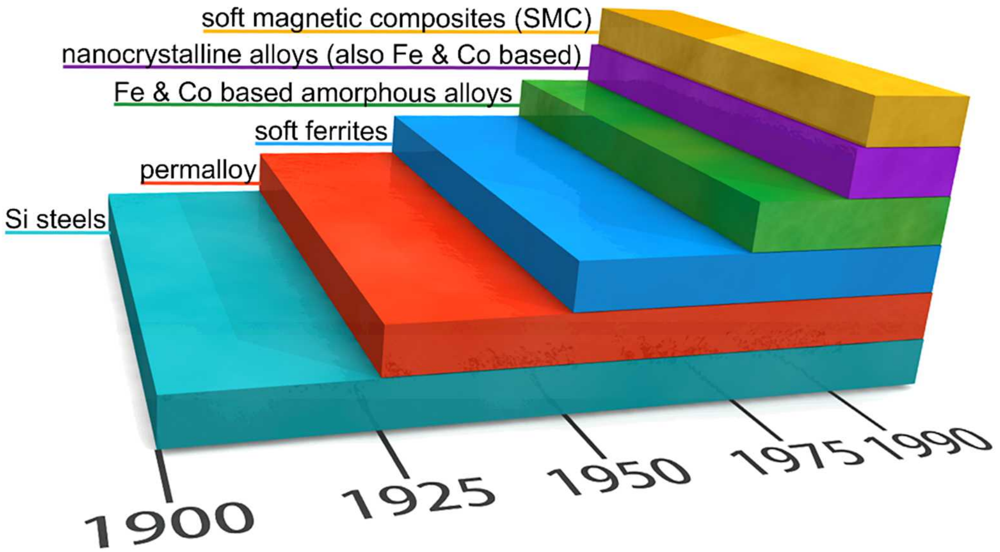

Adapted from: L.A. Dobrzański, M. Drak, B. Ziębowicz, Materials with specific magnetic properties, Journal of Achievements in Materials and Manufacturing Eng., 17, 37 (2006).

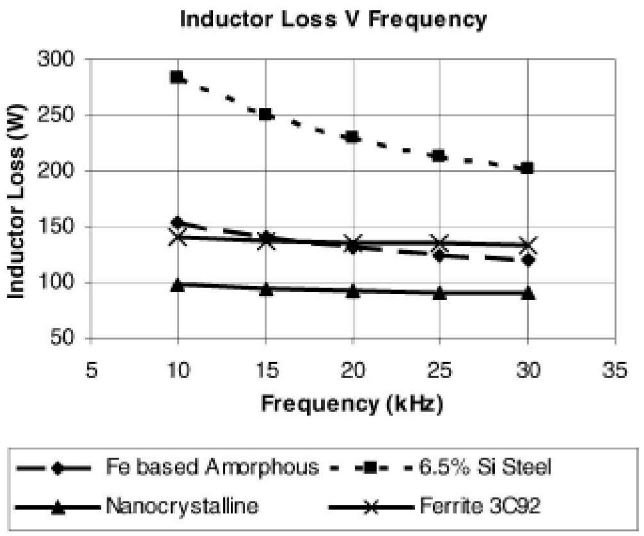

B.J. Lyons, J.G. Hayes, M.G. Egan, Magnetic Material Comparisons for High-Current Inductors in Low-Medium Frequency DC-DC Converters, IEEE, 71 (2007).

Magnetic Material	J_s (T)	$\rho(\mu\Omega\cdot m)$	Cost
VITROPERM (Vacuumschmelze)	1.20	1.15	High
Metglas 2605SC	1.60	1.37	High
Ferrite (Ferroxcube)	0.52	$5x10^6$	Low
Si steel	1.87	0.05	Low
γ'-Fe_4N	1.89	> 200	Low

γ'-Fe_4N

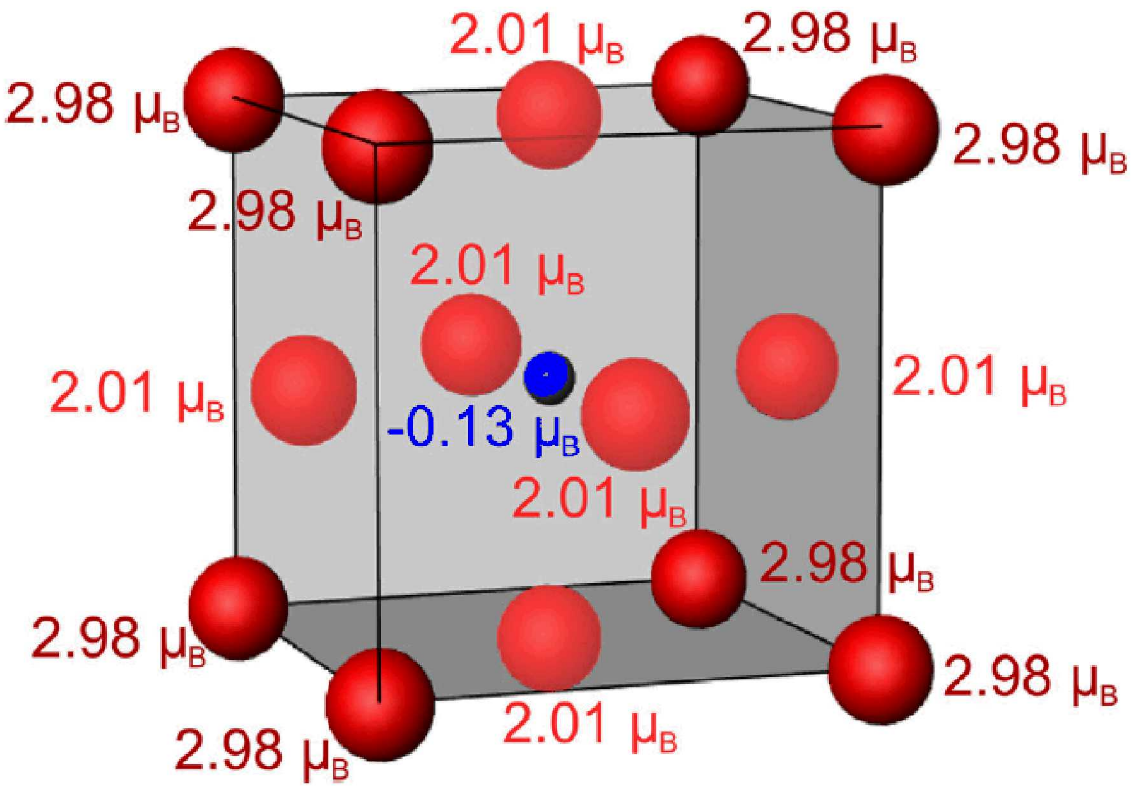

fcc γFe structure stabilized by interstitial nitrogen in the body center

G. Scheunert, et al., A review of high magnetic moment thin films for microscale and nanotechnology
Applications, Appl. Phys. Rev., 3, 011301 (2016).
J.M.D. Coey, *Magnetism and Magnetic Materials* (Cambridge University Press, Cambridge, UK, 2012).

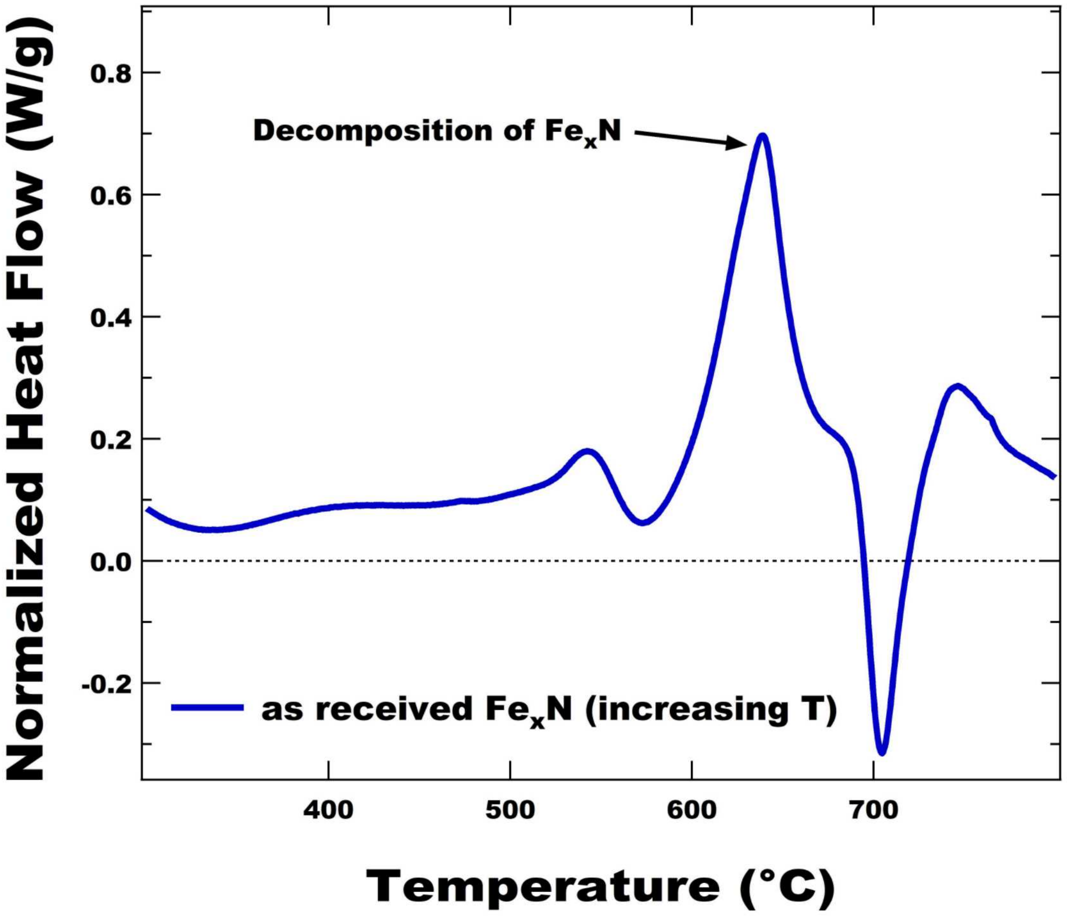

Relatively low thermal decomposition limits consolidation/fabrication methods

Spark Plasma Sintering (SPS)

SPS Model: SPS-825S Dr. Sinter® at UC Irvine

Starting Powder in Die

End Product

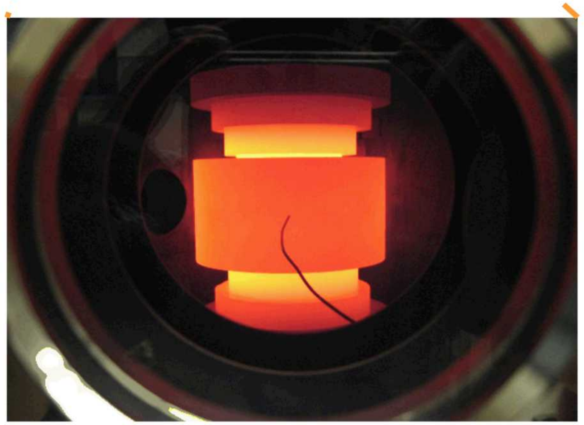

SPS Chamber

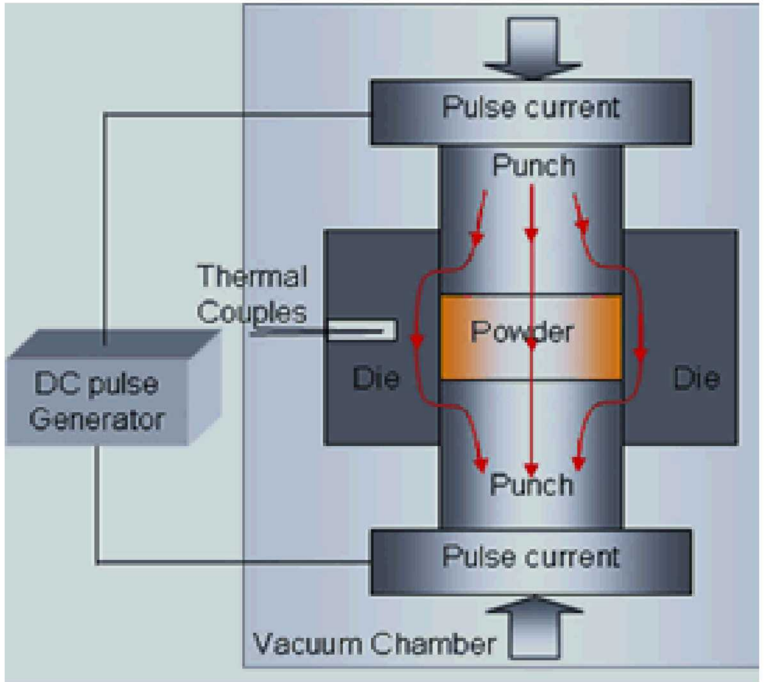

SPS consolidated Iron Nitride

First ever bulk γ'-Fe_4N!

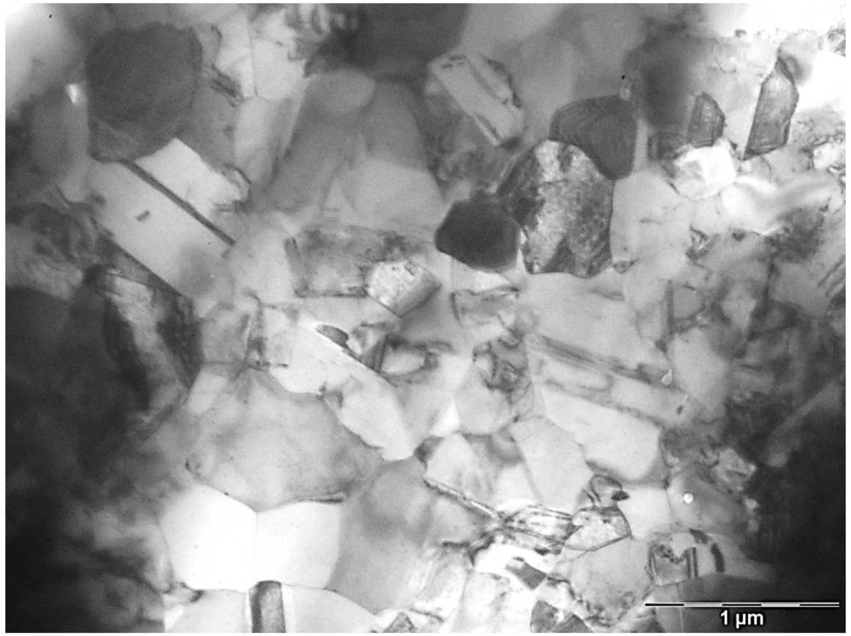

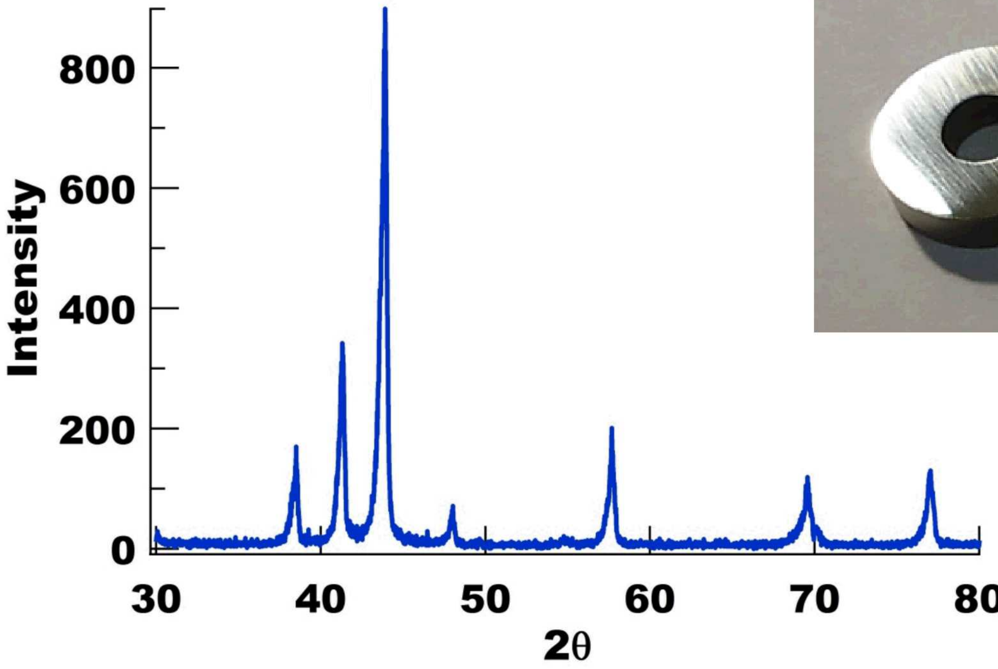

Net-shaped toroid (no machining required)

- **Fe nitride powders well consolidated with little porosity**
- **Grain sizes 200 nm – 1 µm → fine grain size = low H_c**
- **γ'-Fe_4N primary phase**
- **Fe_3N secondary phase from mixed phase starting material**

Toroid Surface SEM and EDS

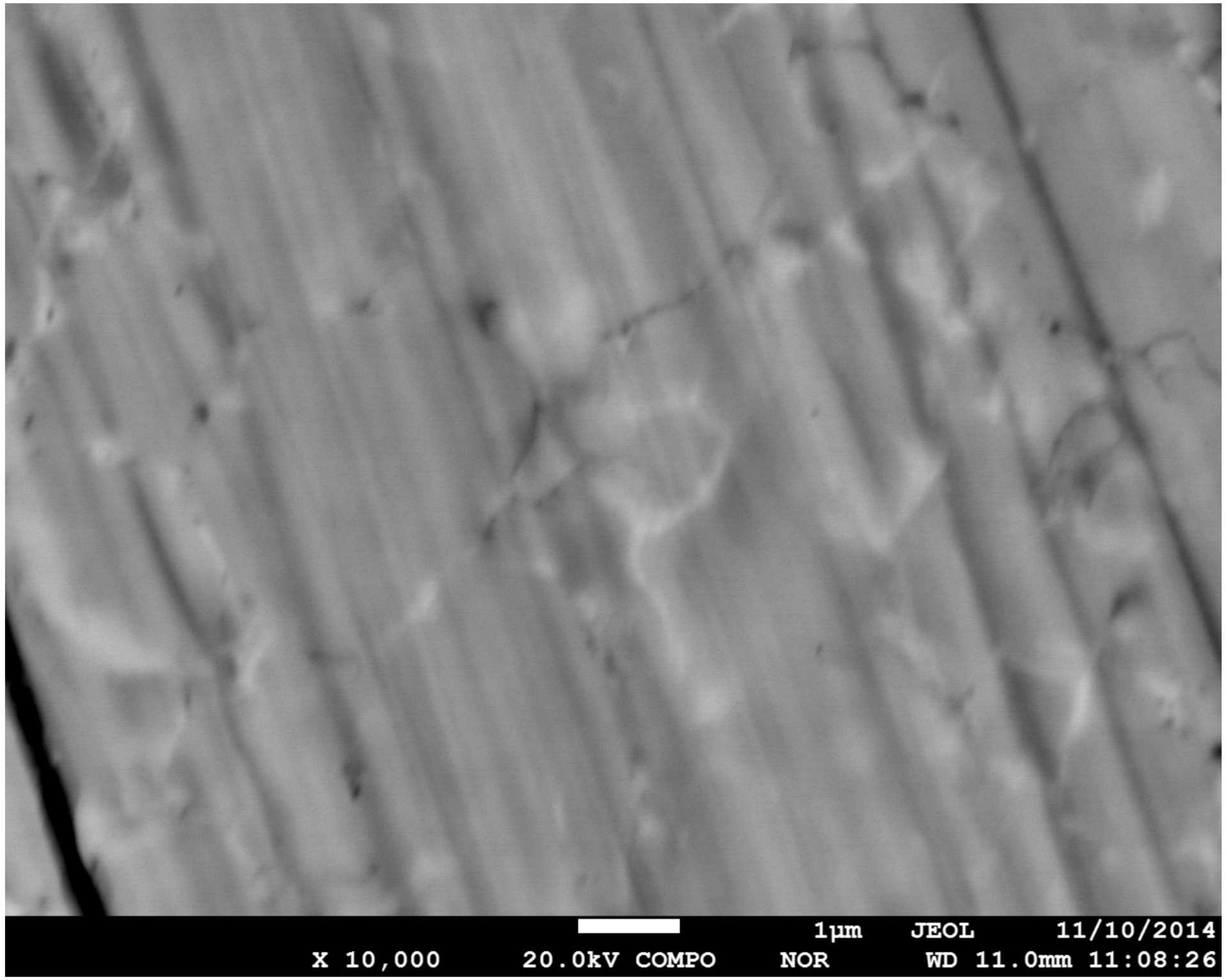

Location	Fe (Atomic %)	N (Atomic %)
Grain center	81.3	18.7
Grain boundary	84.2	15.8

- **Small variation in composition between grain boundary and center**
- **Grain center stoichiometry ≈ Fe_4N**
- **Grain boundary is ≈ 3 Atomic% richer in iron**

*SEM/EDS analysis completed by Dick Grant (SNL)

γ'-Fe_4N Synthesis and Processing

U.S. Patent Issued (#9,963,344)

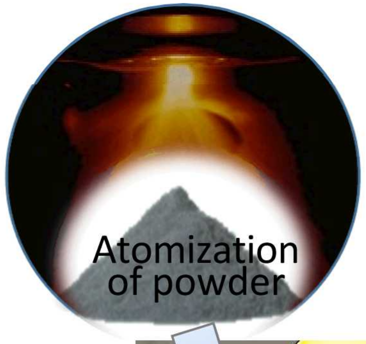

Cryomilling
Severe Plastic deformation

Fluidized Bed Furnace

SPS Consolidation

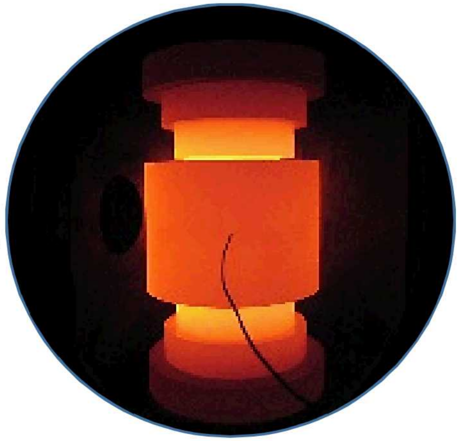

Spark Plasma Sintering
Fast sintering

- **Pressure and pulsed current assisted sintering process**
- **Precision control over heat, pressure, and time**
- **Restrain grain growth**
- **Full densification**

Magnetic Characterization

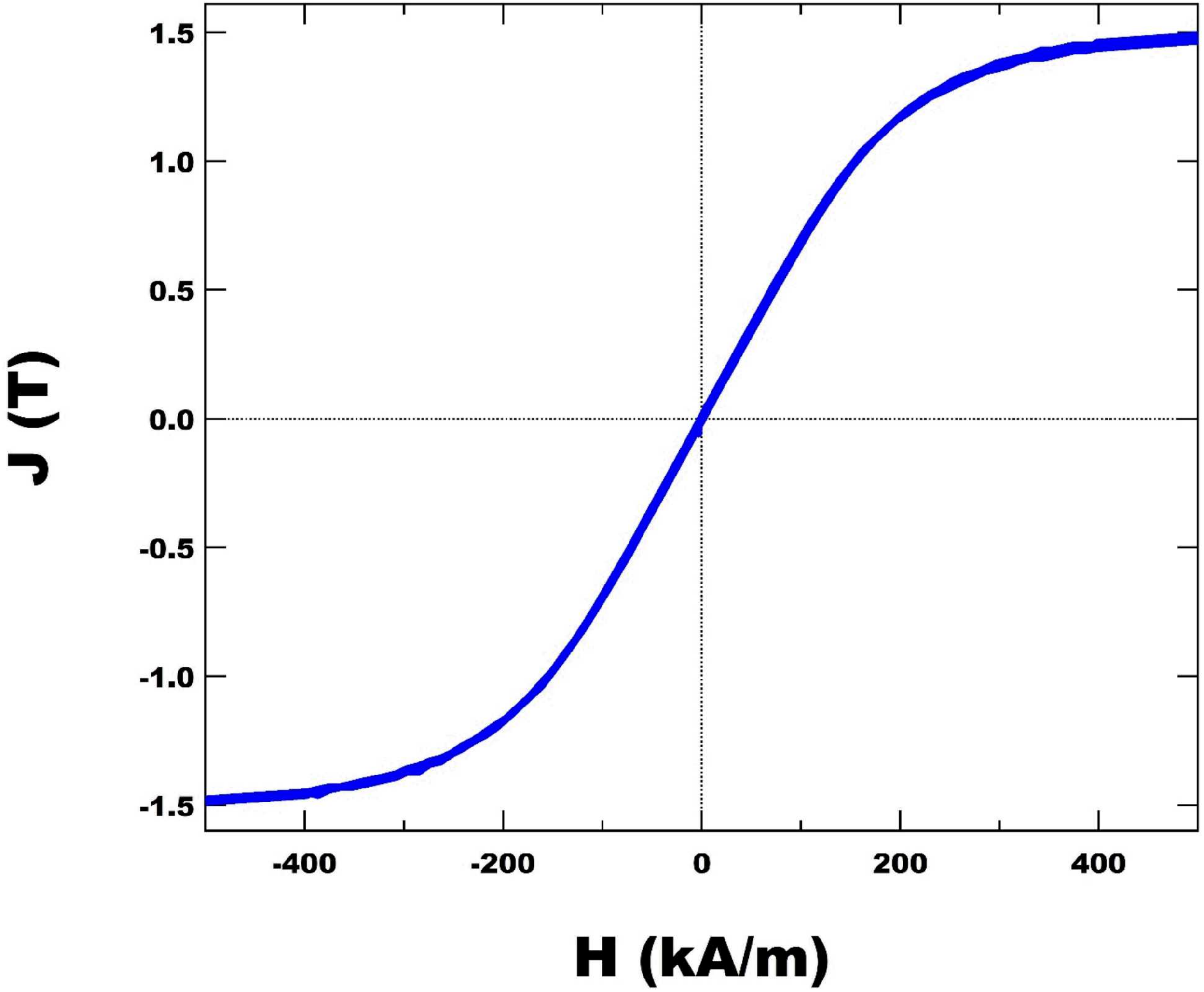

- SPSed at 550°C and 100 MPa
- J_s = 1.62 T
- Theoretical J_s = 1.89 T
  - (SiFe is 1.87 T)
- H_c < 1000 A/m

SEM of SPSed FeN samples, (Ø5mm, 525^{o}C, 200MPa)

W/ as-received FeN powder

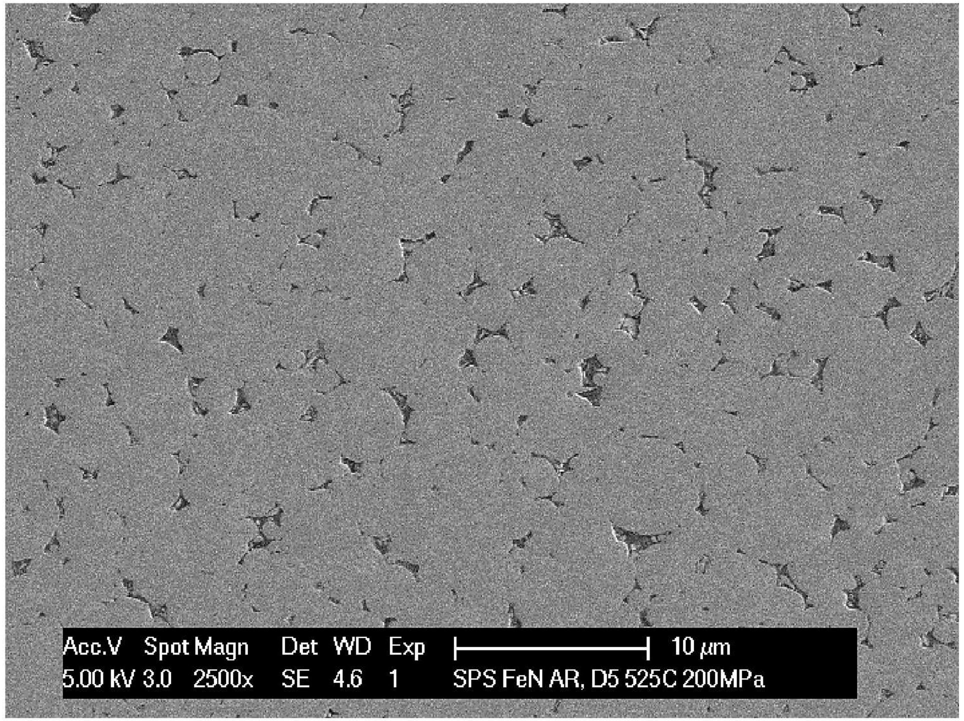

W/ milled FeN powder

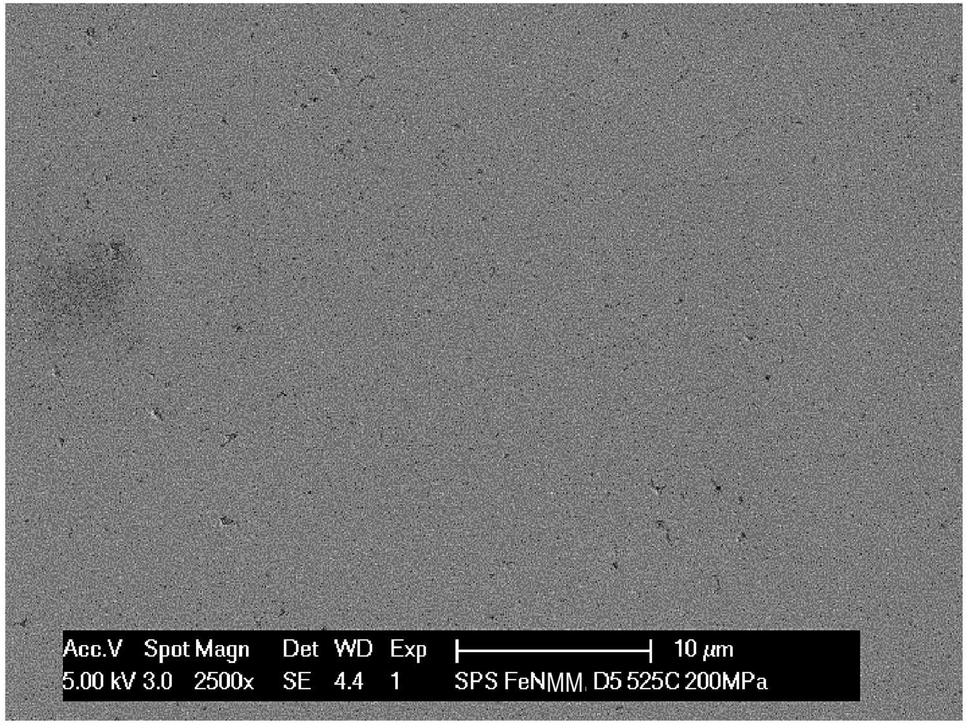

- **Milled FeN powder produces more uniform and dense SPSed billets**
  - **Higher packing density with smaller particle size**
  - **Enhanced diffusion with smaller grain size of milled powder**

Density of SPSed Fe_4N samples

$\rho_{theory} = 7.212\ g/cm^3$

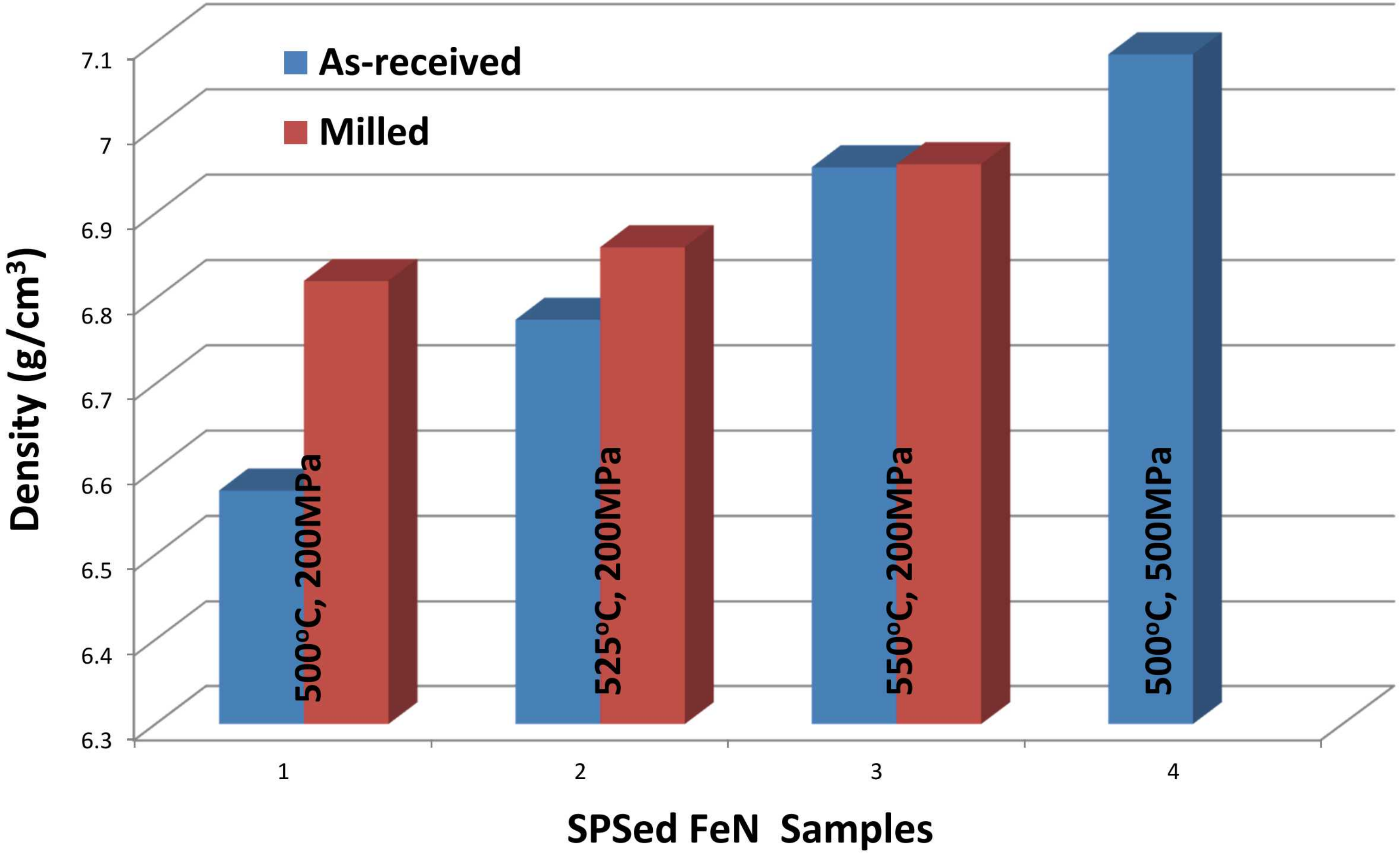

- **Density increases with increasing SPS temperature and pressure**
- **Milling improves both density and sample uniformity**

Grain Size, Domain Wall Motion, and Coercivity

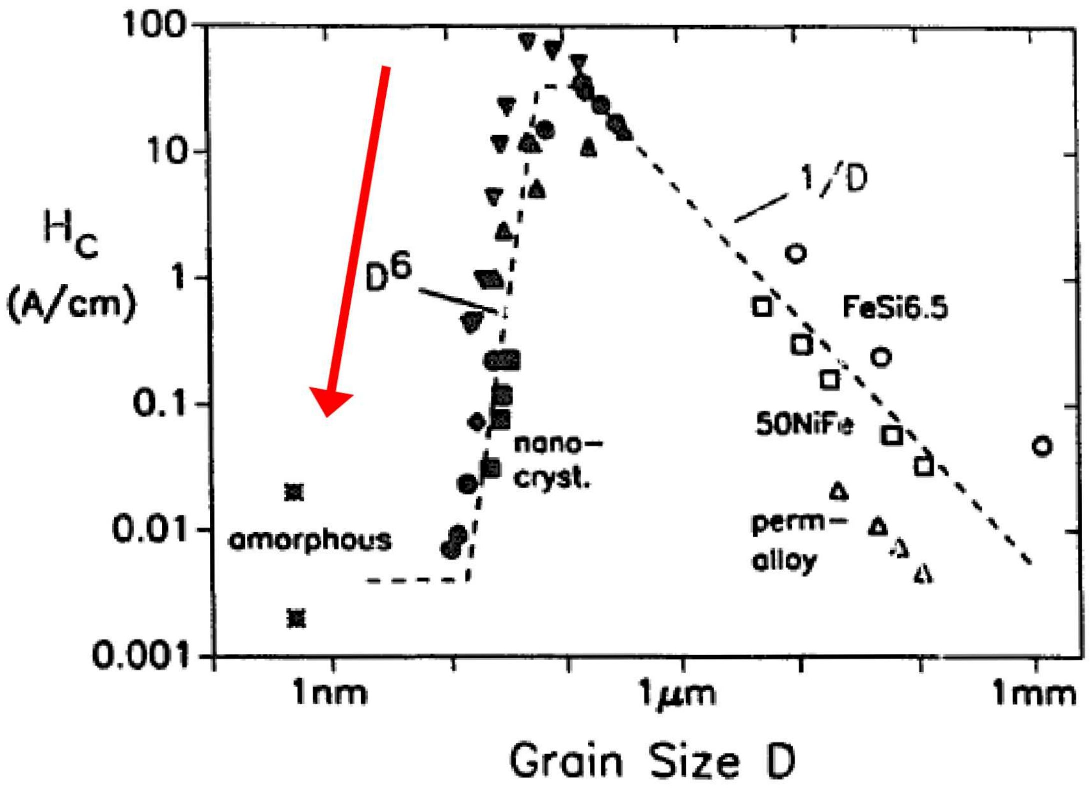

Fig. 2. Coercivity H_c vs. grain size for various soft magnetic metallic alloys. The data of the nanocrystalline material refer to (▲) FeNbSiB and (●) FeCuNbSiB [14], (◆) FeCuVSiB [15], (■) FeZrB [4] and (▼) FeCoZr [16].

G. Herzer, Nanocrystalline Soft Magnetic Materials, J. Magn. Mag. Mat., 112, 258 (1992).

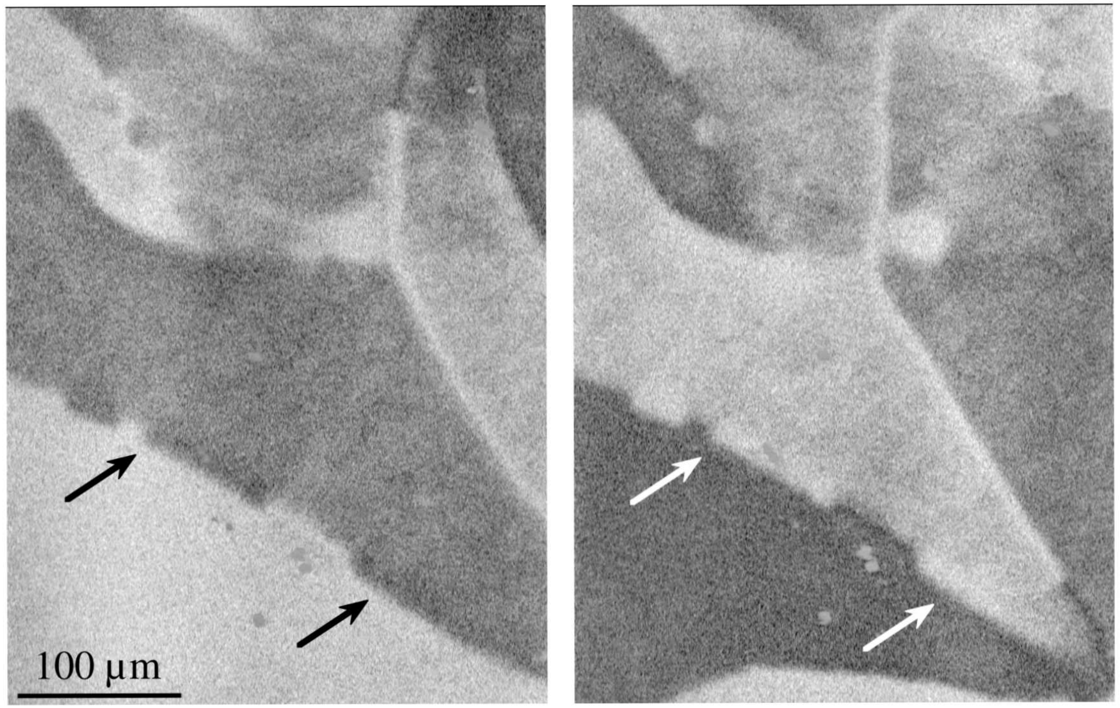

R. Schaefer and G. Herzer, "Continuous magnetization patterns in amorphous ribbons," IEEE Transactions on Magnetics, vol. 37, pp. 2245-2247, 2001.

Synthesis of Fine Grained Iron Nitride

$$\text{Fe nanoparticles} \xrightarrow[NH_3\ (l)]{} Fe_xN$$

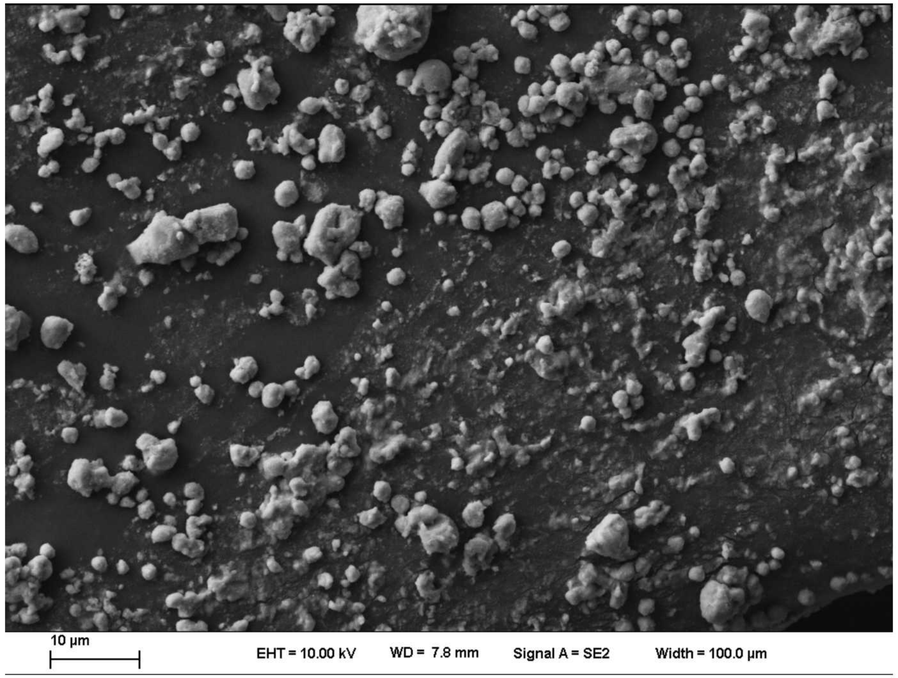

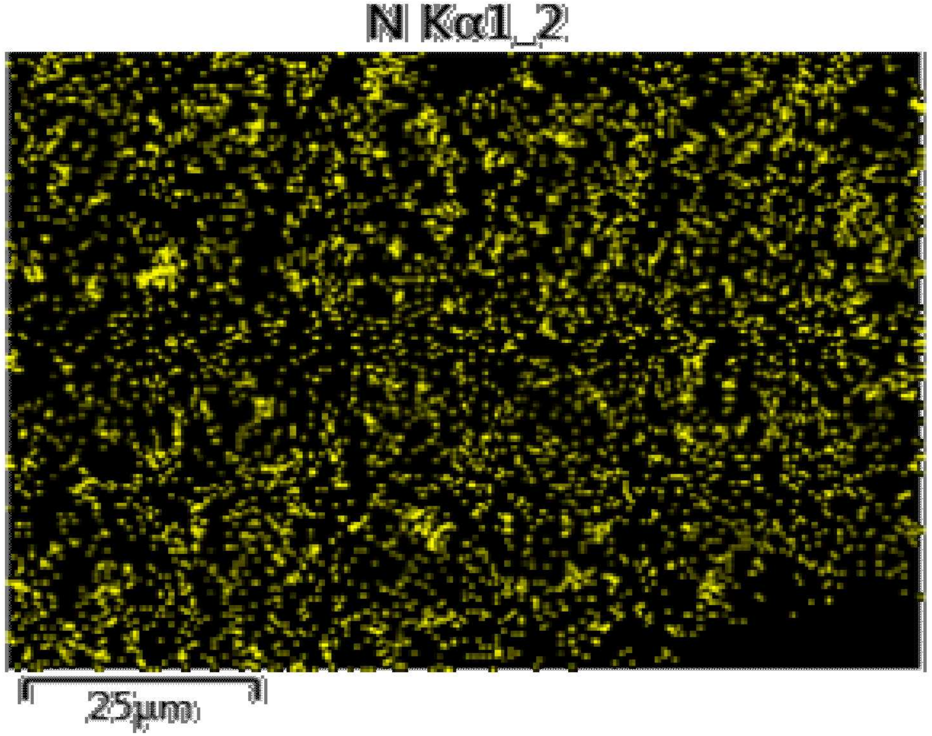

- SEM-EDS confirms nitrogen content
- Optimizing process
- Additional routes being investigated

Ferroelectrics (Barium Titanate)

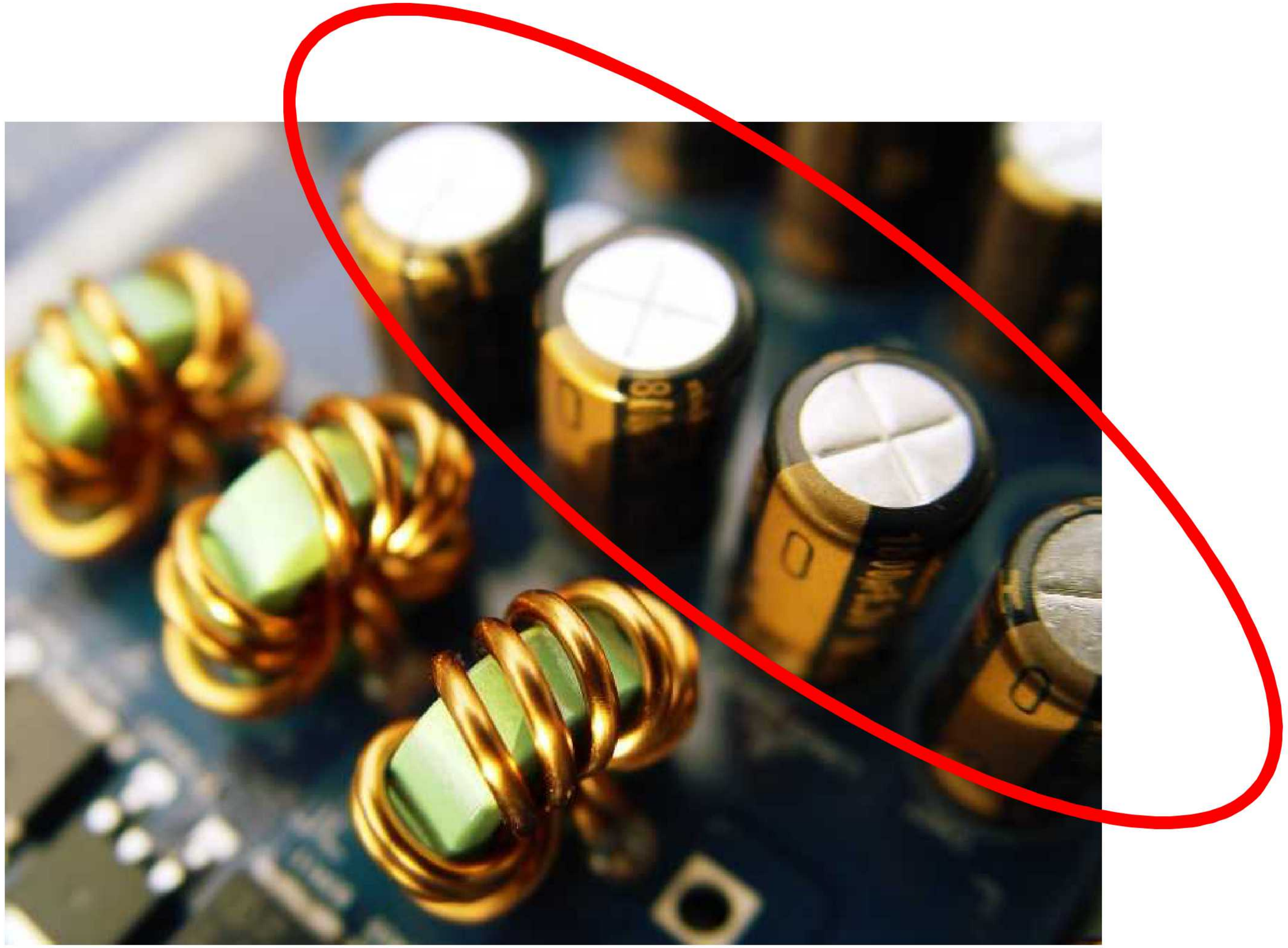

Capacitor Needs for Storage

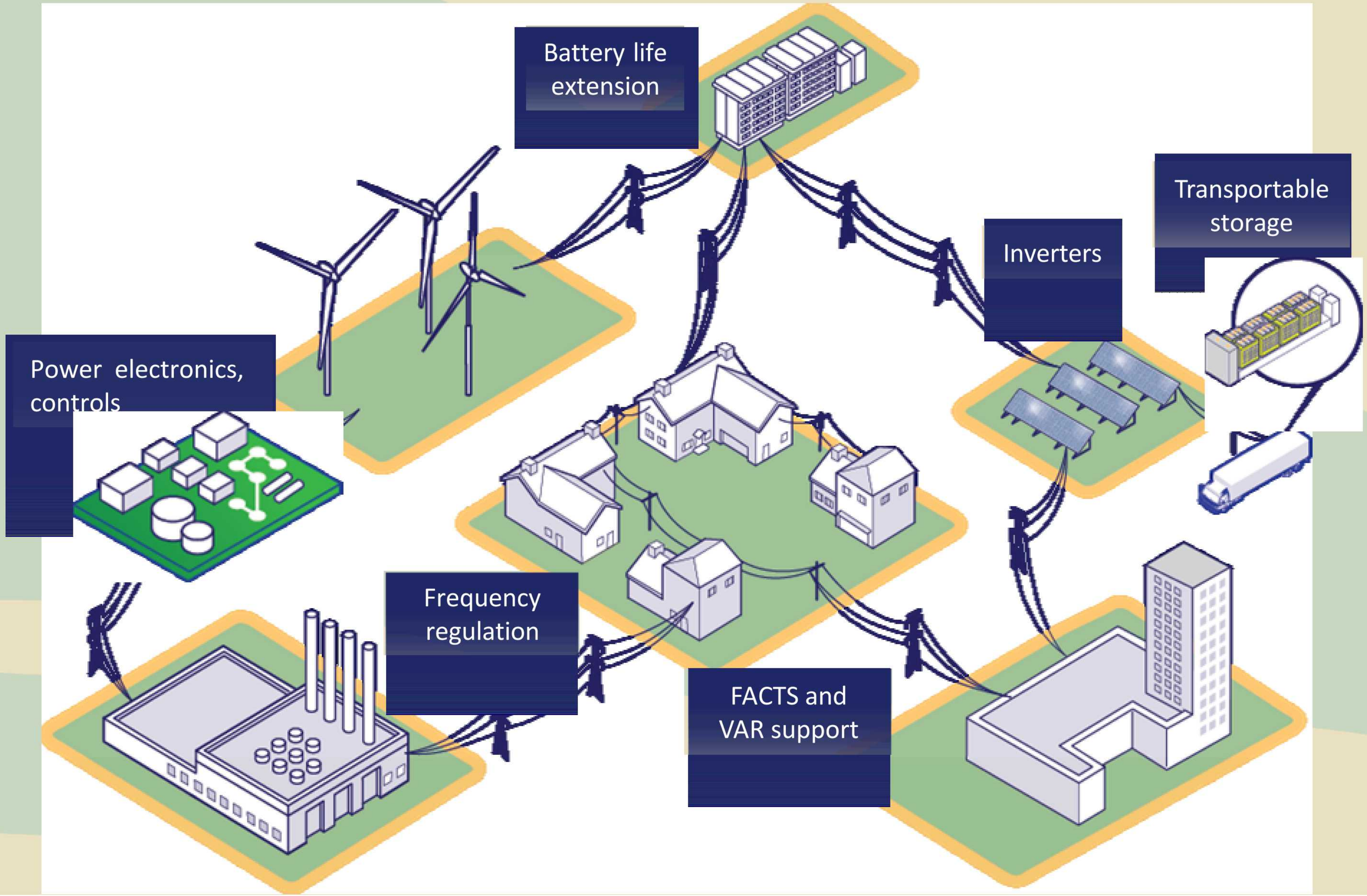

Benefits of Nanocrystalline Ferroelectrics

- **Permittivity may increase with decreasing grain size down to a critical size dimension (higher energy density)**
- **High frequency performance improves with decreasing grain size (maintain permittivity and low loss to higher frequencies)**
- **Field and temperature dependence of permittivity may improve (i.e. lower TCC and VCC)**

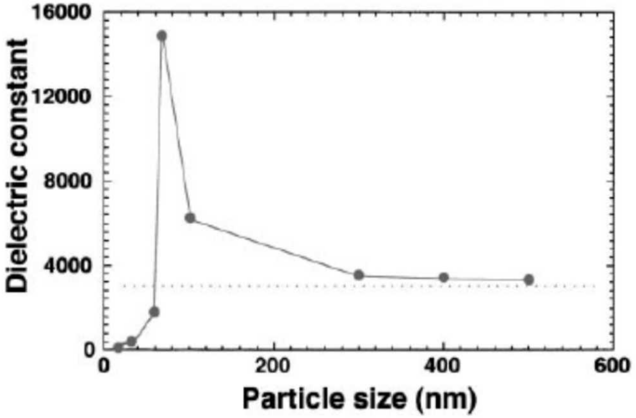

$BaTiO_3$ particles in solution

Wada et. al., Jpn. J. Appl. Phys. Vol. 42 (2003) 6188–6195

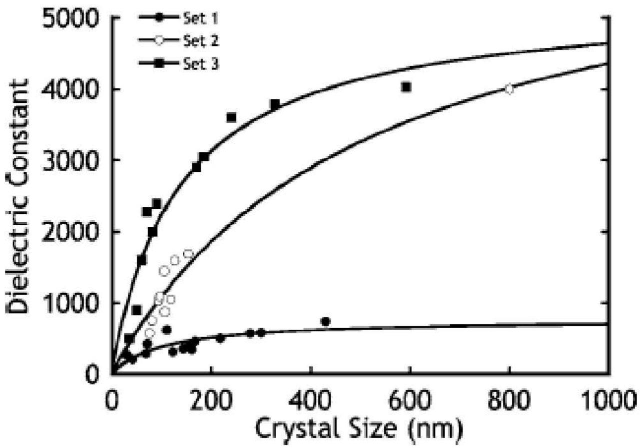

Sintered $BaTiO_3$

Aygün et. al., J. Appl. Phys. Vol. 109 (2011) 034108

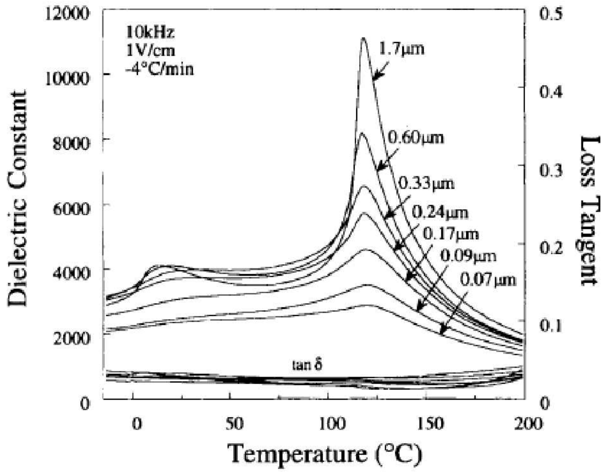

Frey, et. al., Ferroelectrics, Vols. 206-207, (1998) 337-353

Most widely reported and agreed upon behavior

Benefits of Nanocrystalline Ferroelectrics

- **Nanocrystalline grain size provides high breakdown strength (BDS)**
- **Lower field-induced strain (i.e., better electromechanical performance)**

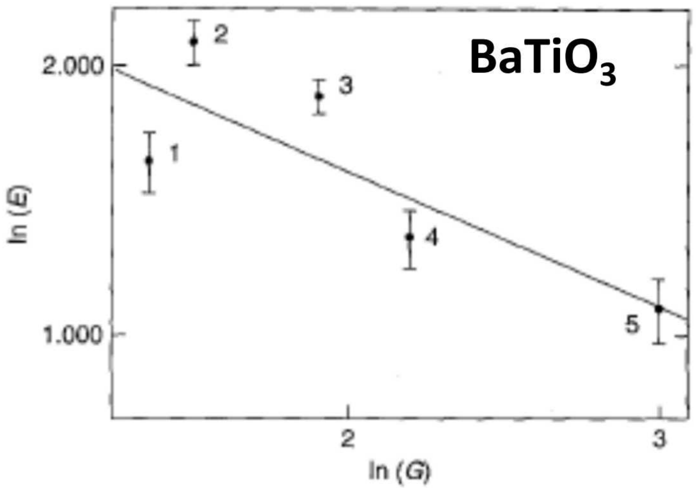

Figure 2 Grain size dependence on dielectric strength. Numbers indicate sintering temperatures: (1) 1320 °C, (2) 1330 °C, (3) 1350 °C, (4) 1380 °C, (5) 1400 °C.

TUNKASIRI, JOURNAL OF MATERIALS SCIENCE LETTERS 15 (1996) 1767-1769

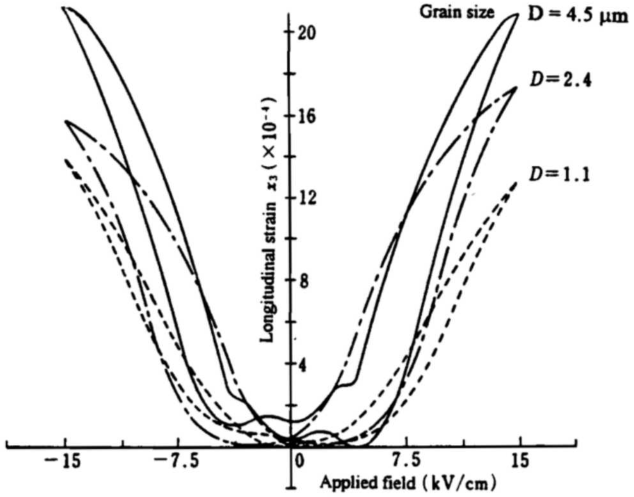

Fig. 3.28 Grain size dependence of the induced strain in PLZT ceramics.

from Kenji Uchino's book, Ferroelectric Devices

Barium Titanate ($BaTiO_3$ or BTO)

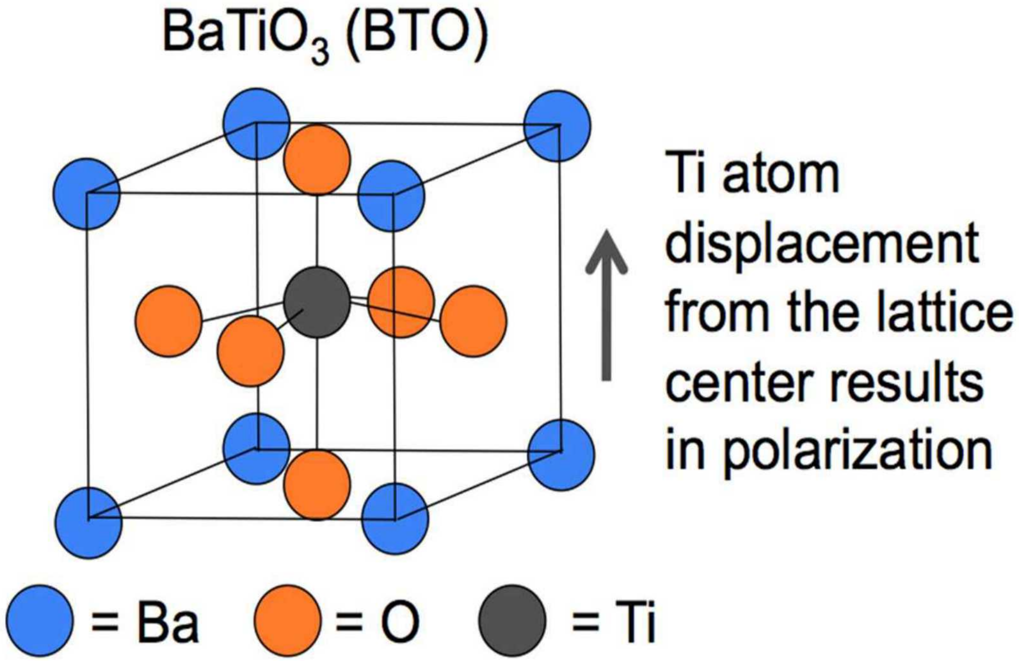

(Perovskite Structure)

- **Ferroelectric in bulk at room temperature**
- **High dielectric constant**
- **Wide variation in reported nanoparticle dielectric constants**

Device Fabrication

Sintering

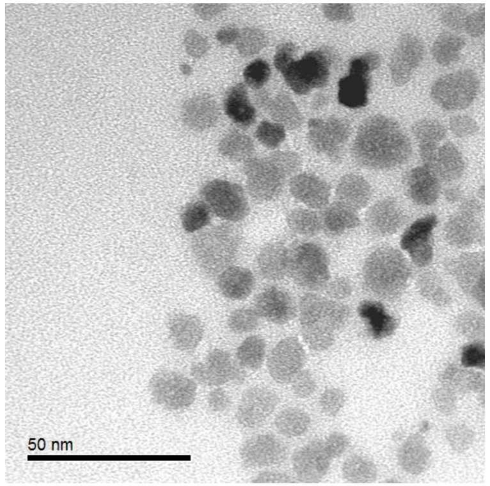

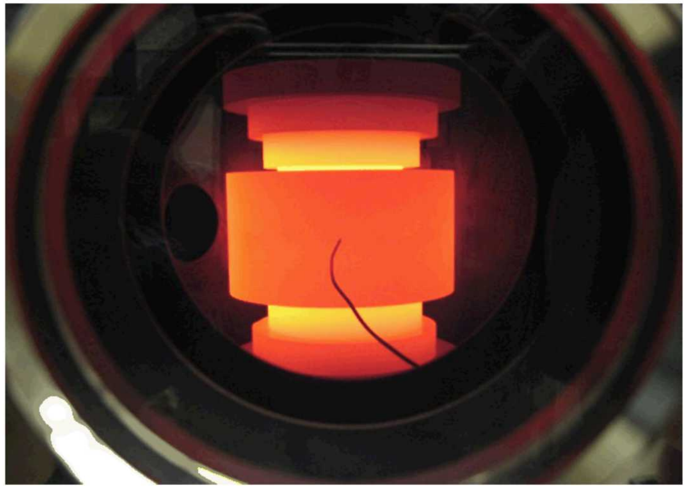

Spark Plasma Sintering die

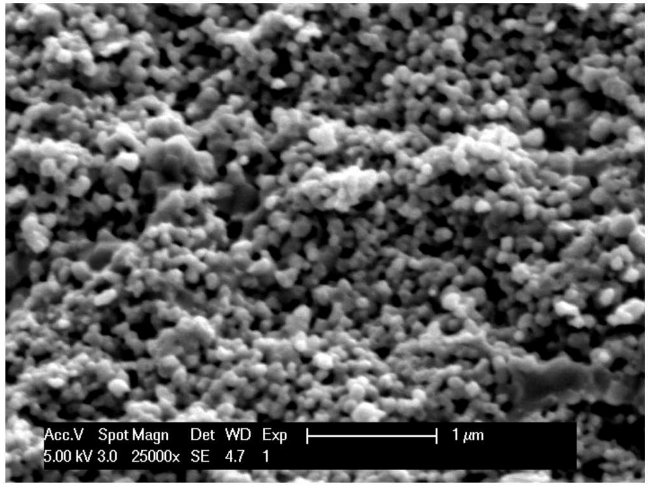

SNL BTO, grain size 100 – 200 nm

Polymer composite

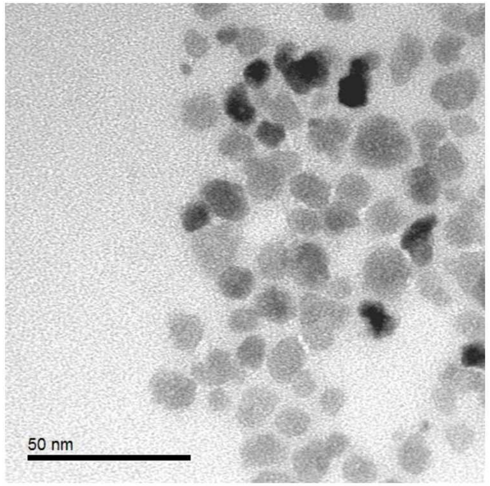

+

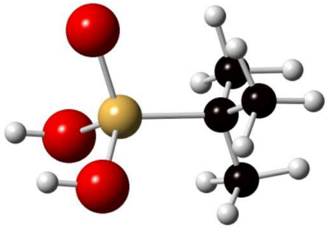

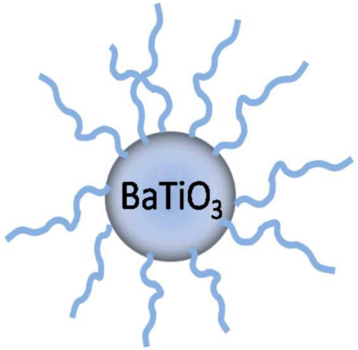

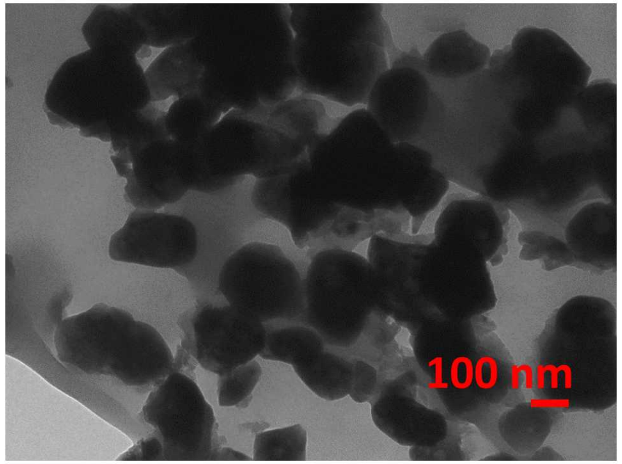

Benefits of SPS

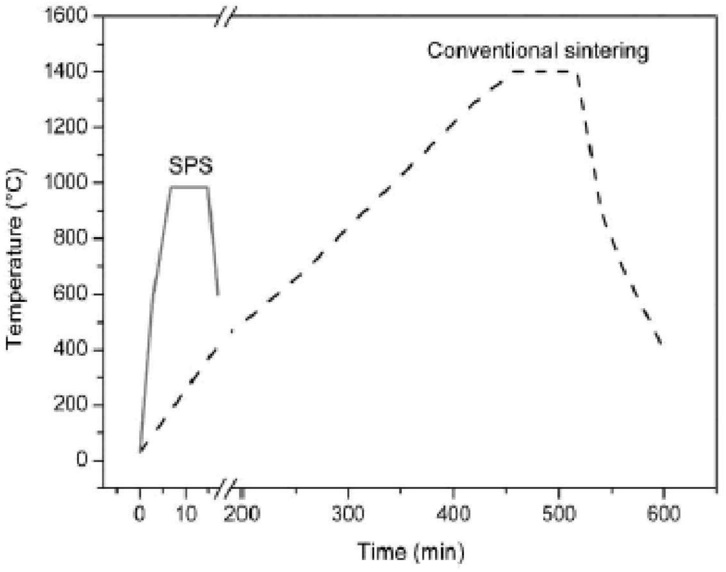

Fig. 4. Comparison of sintering profiles of $BaTiO_3$ ceramics obtained by conventional sintering and by SPS.[10]

Hungría et. al., Adv. Eng. Mater. Vol. 11 (2009) 616.

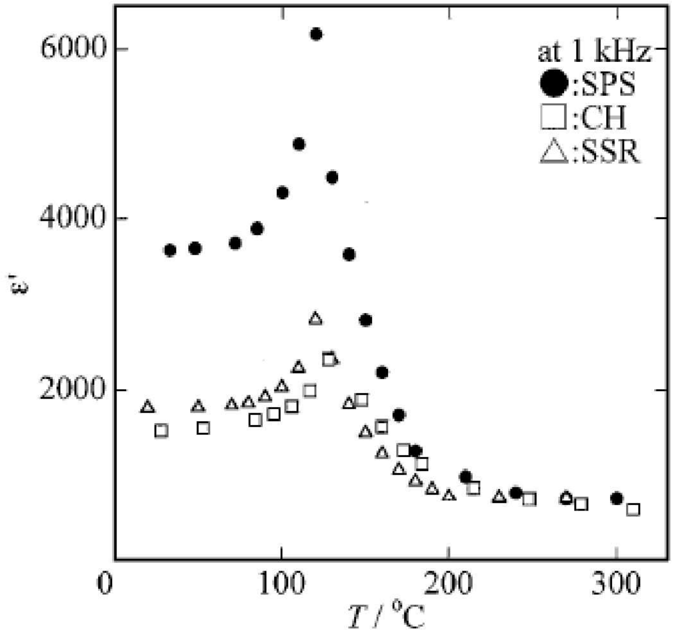

Figure 5 Temperature dependence of the permittivity at 1 kHz for SPS, CH and SSR $BaTiO_3$ pellets.

Takeuchi et. al., J. Mater. Sci. Vol. 34 (1999) 917.

- **Dramatically shorter overall sintering times**
- **Lower sintering temperatures, shorter hold times**
- **Ability to limit/control grain sizes**
    - **Porosity and oxygen defects minimized at same time**
- **Effective in removing resistive grain boundary component**
- **Improved frequency response**

Examples of SPSed BTO

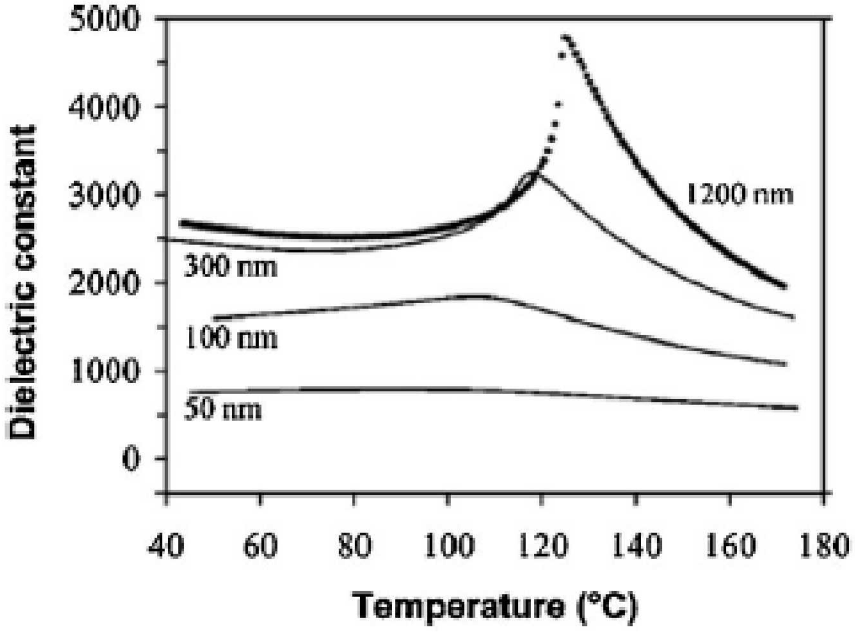

Zhao et al., Phys. Rev. B Vol. 70 (2004) 024107.

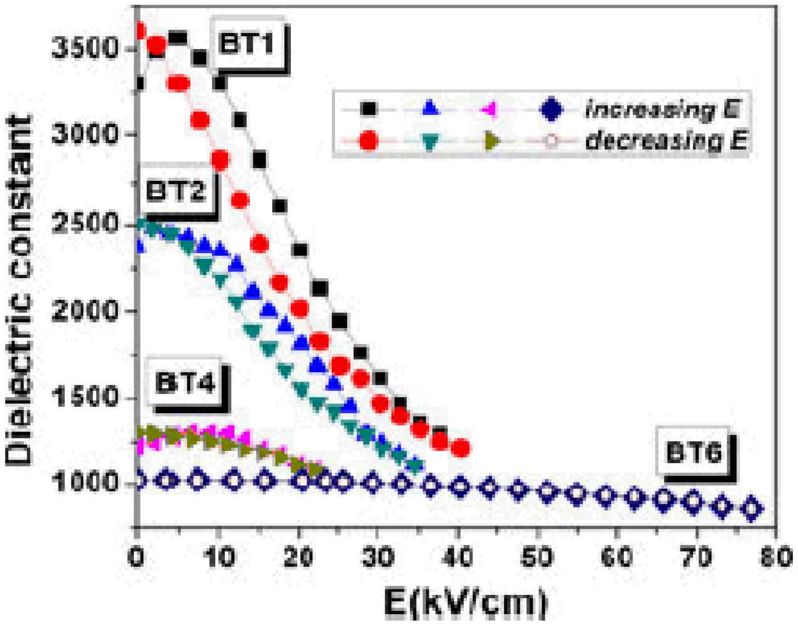

Curecheriu et al., J. Am. Ceram. Soc. Vol. 95 (2012) 3912.

- **Uniform control over grain size allows additional tuning of properties difficult to demonstrate via conventional sintering**
  - **Field dependence of permittivity (VCC)**
  - **Temperature dependence of permittivity (TCC)**

Commercial BTO Nanoparticles

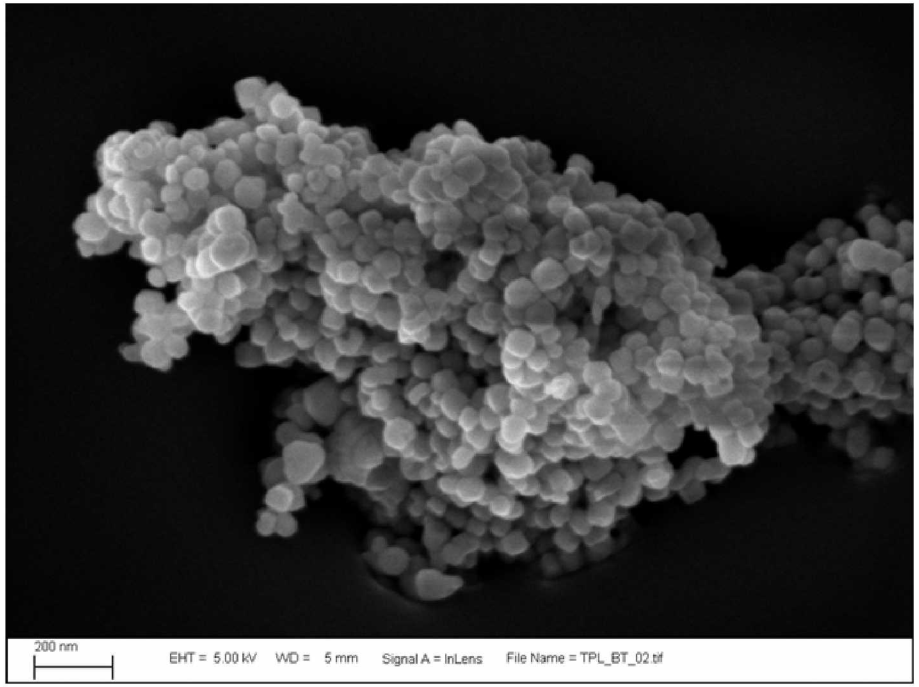

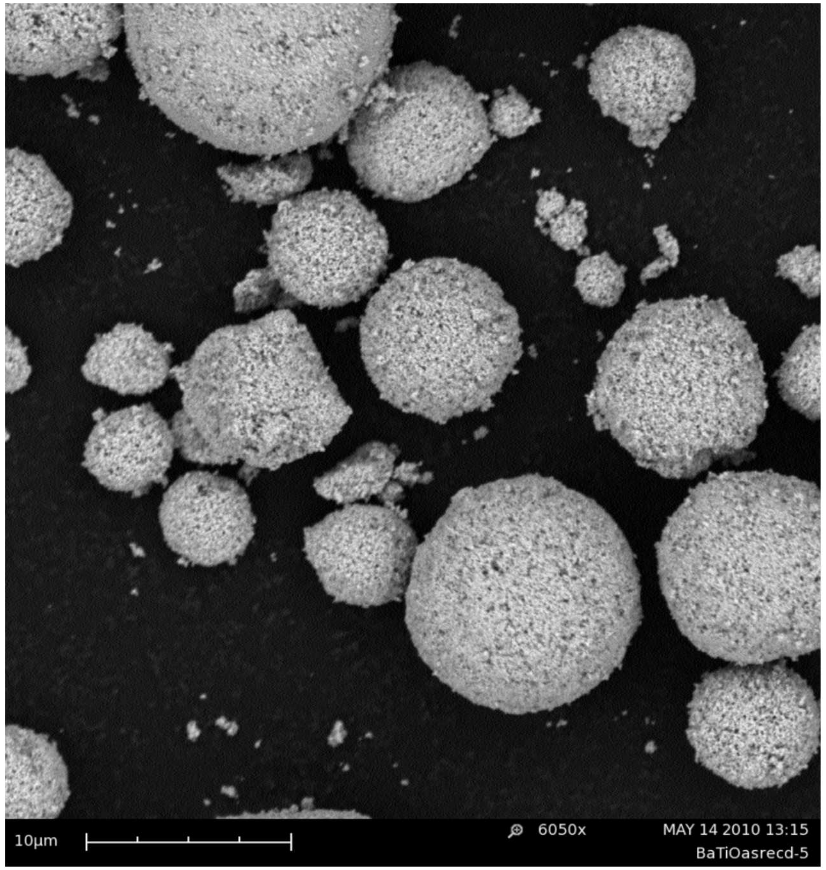

- **NanOxide HPB-1000 from TPL**
- **BET surface area of 16.26 ± 0.0669 m^2/g**
- **60-80 nm primary particle size**
- **1-20 µm "soft" agglomerates**

Abnormal Grain Growth

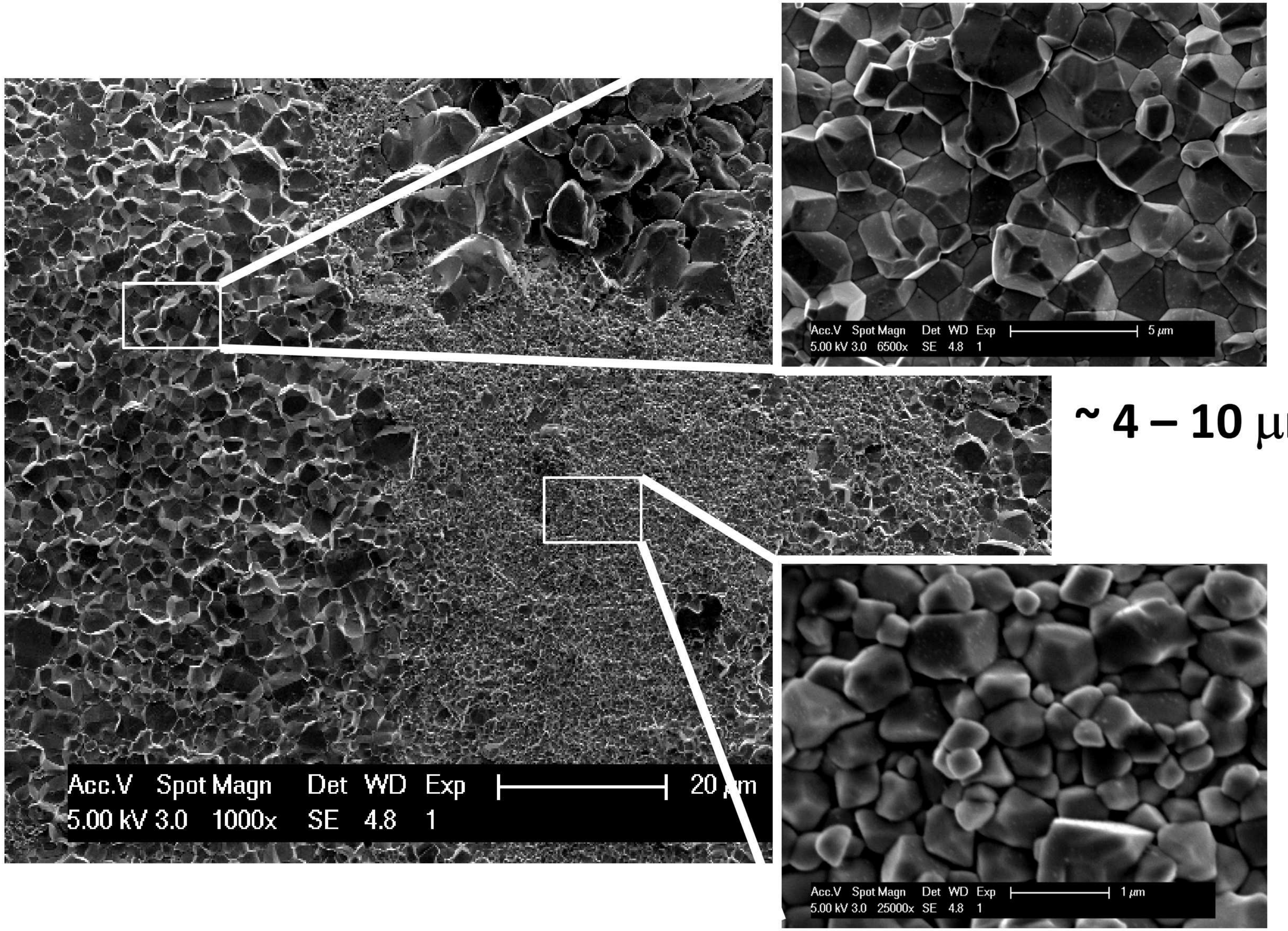

~ 4 – 10 μm

~ 500 nm

1000 °C, 6 min. hold

Abnormal Grain Growth

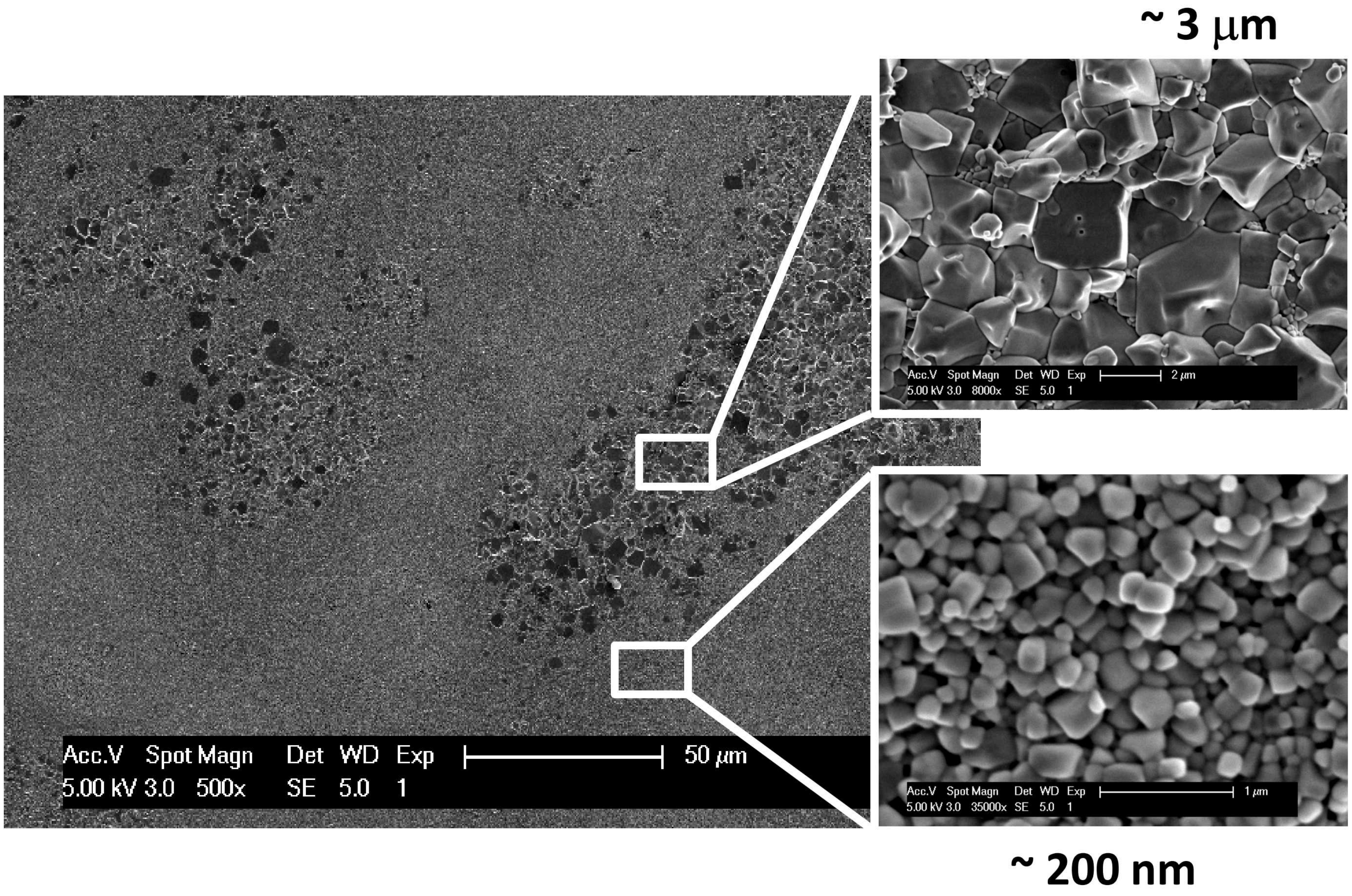

950 °C, 3 min. hold

SNL BTO Nanoparticle Synthesis

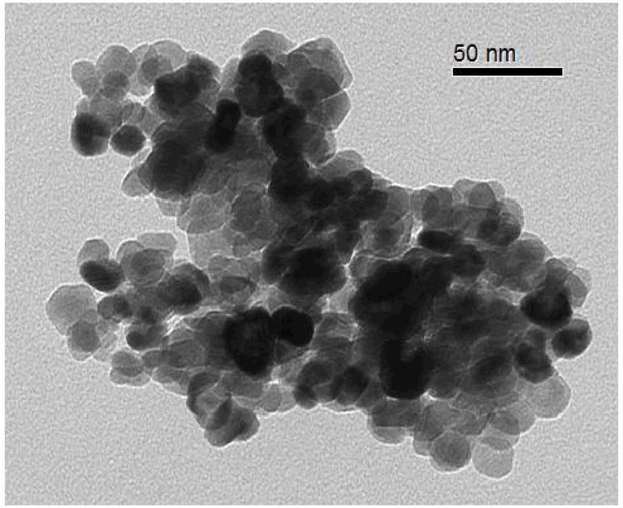

~ 10 nm diameter

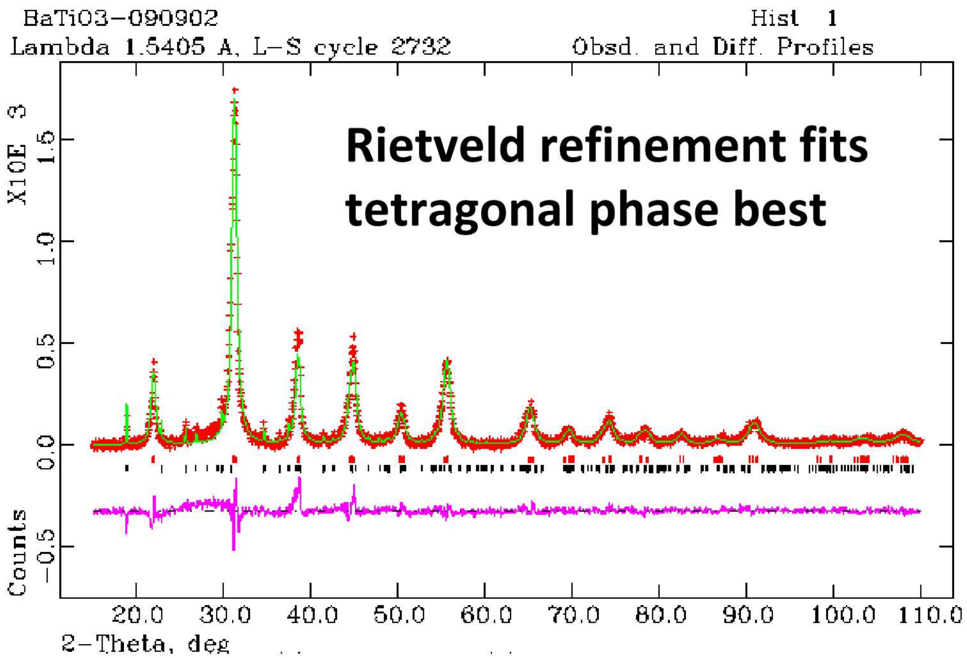

- **$Ba(OH)_2 \cdot 8H_2O$ and $Ti(OPr)_4$ precursors at 80 ˚C**
- **Redesigned synthesis with air-free chemistry and improved control over water addition**
- **Rietveld analysis fits tetragonal phase when particles synthesized with 0.5 and 0.6 mol H_2O**

Yoon et. al., *J. Am. Ceram. Soc.* 90 311 (2007)

BTO size effects as seen in XRD

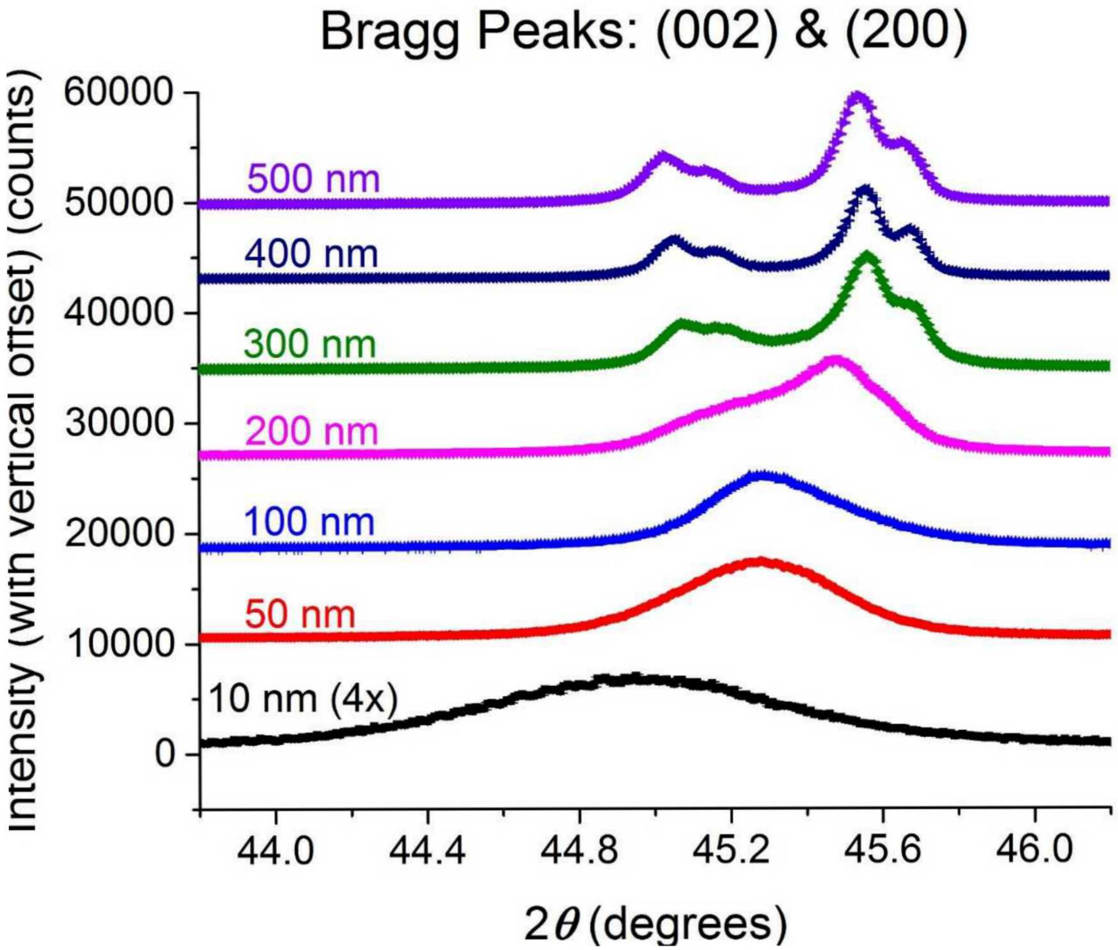

- **Large BTO NPs (bulk) have split peaks!**
- **Small BTO NPs have singlet peaks!**
- **200 nm BTO NPs are on the fence!**

Shi, et al., “Barium titanate nanoparticles: Short-range lattice distortions with long-range cubic order," Phys. Rev. B., vol. 00, pp. 005400, 2018.

Particle Size Dependent Behavior

Synchrotron aPDF (atomic pair distribution function) Analysis

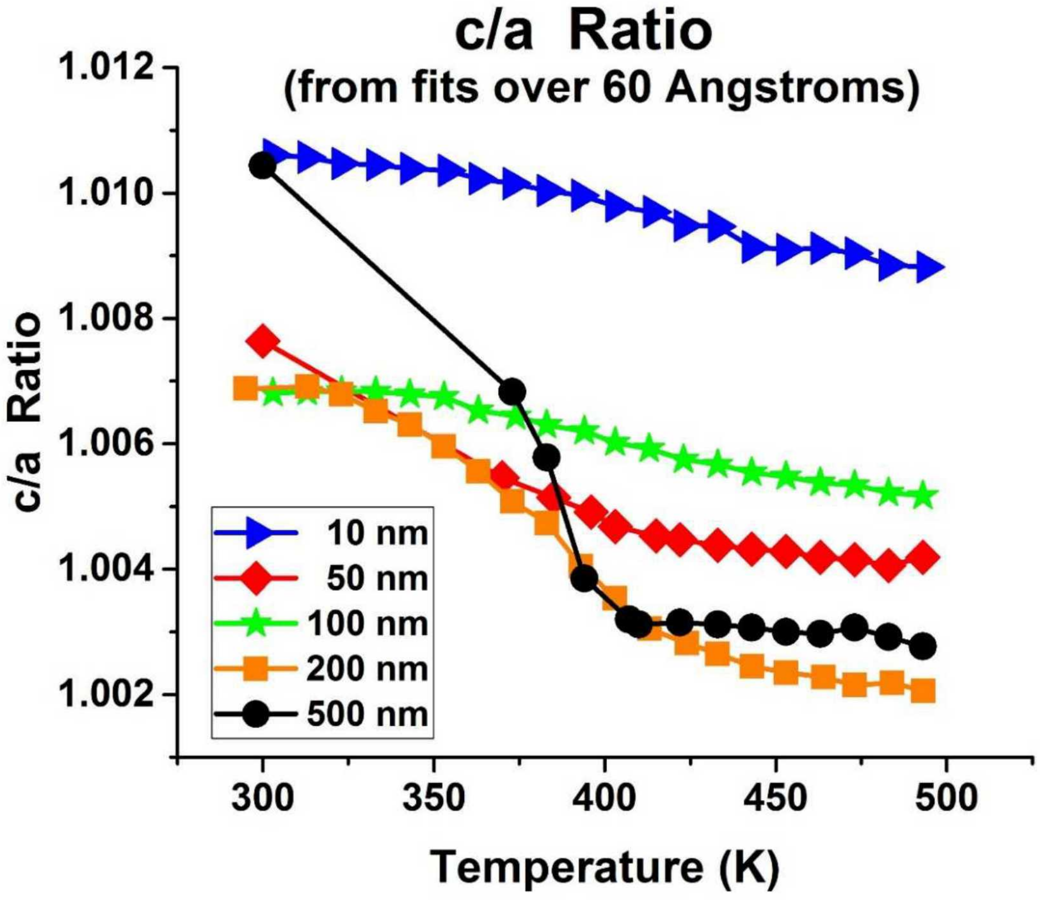

< 120 °C (393.15 K)

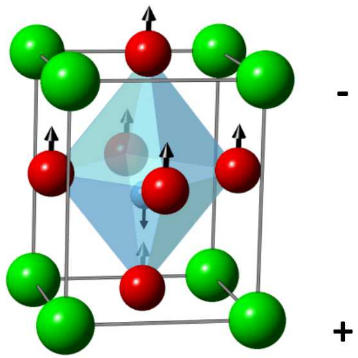

Tetragonal (Ferroelectric)

> 120 °C (393.15 K)

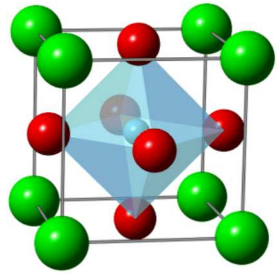

Cubic (Paraelectric)

Synchrotron X-ray data collected at NSLS at Brookhaven National Lab

Raman of SNL BTO (unsintered)

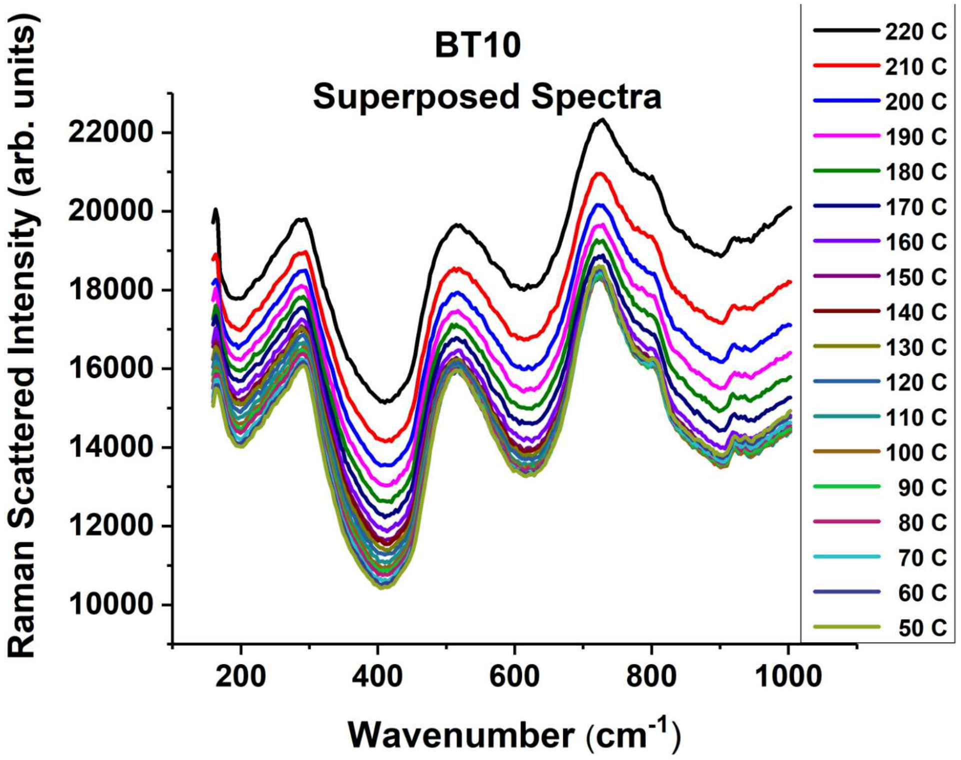

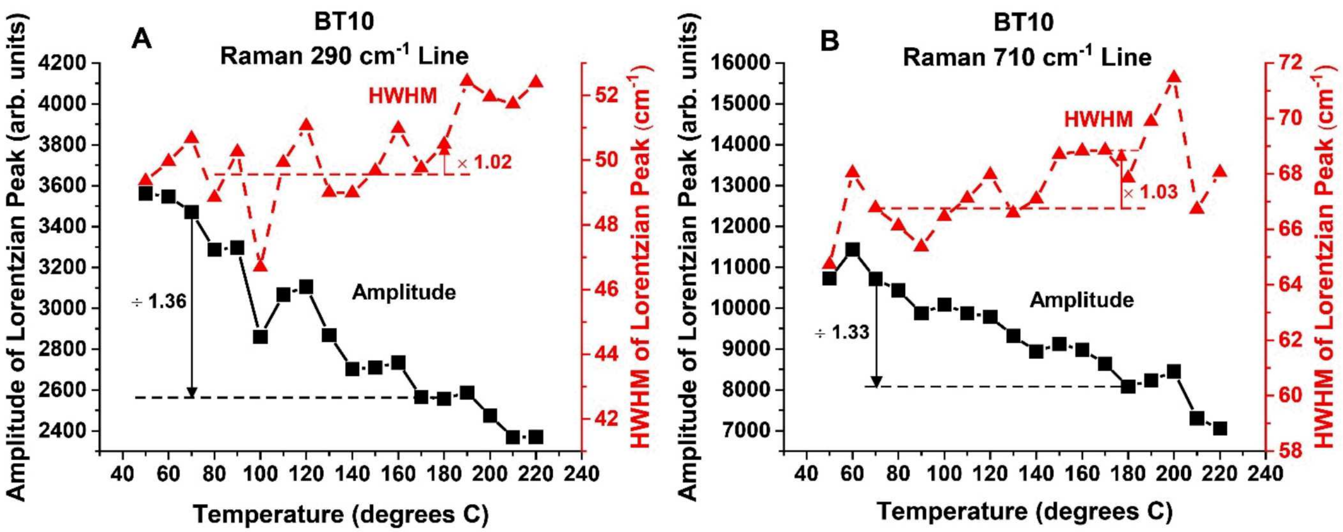

- **290 cm^{-1} and 710 cm^{-1} persist above the Curie temp. (120 °C)**
- **Raman lines are very broad and sit above a temp.-dependent background**

Sintering of SNL BTO Nanoparticles

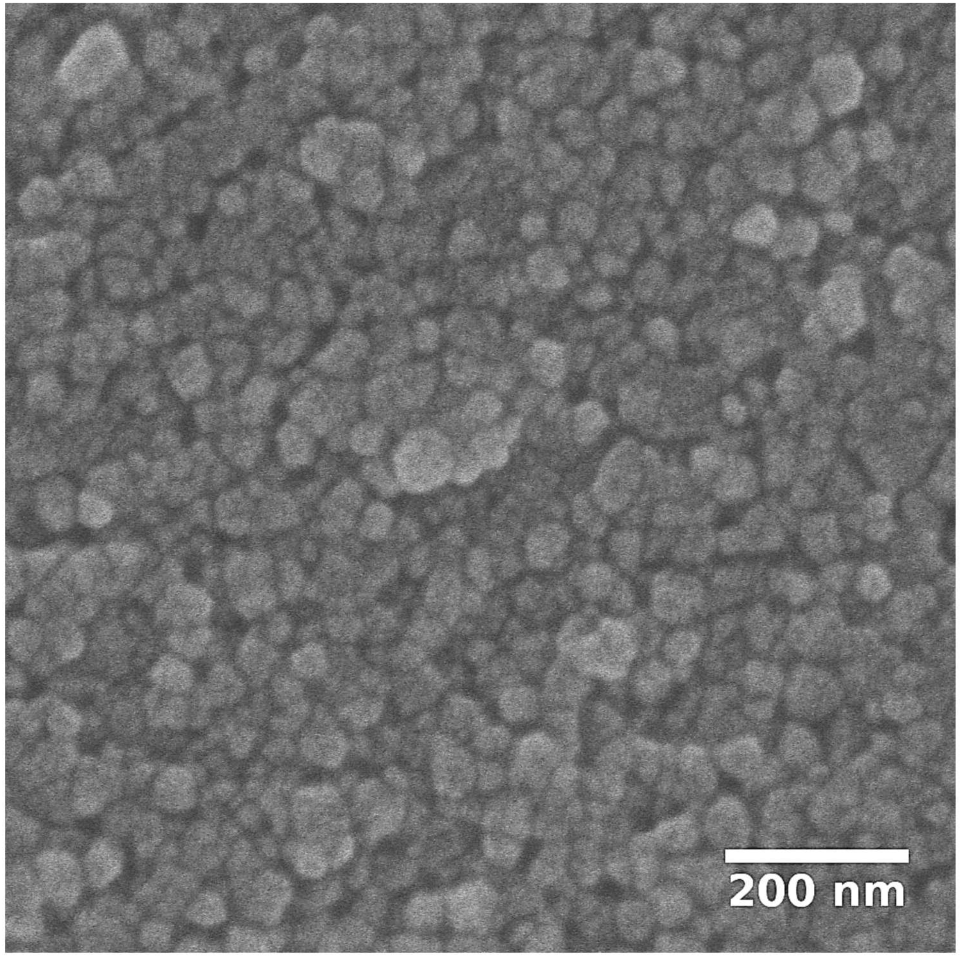

- 800 °C sintering temp.
- 1.4 GPa sintering pressure
- 5 hr. anneal at 700 °C
- $\rho = 5.98\ g/cm^3$
  - 99.7% of theoretical
- 20 – 40 nm grain size

Permittivity vs. Temperature

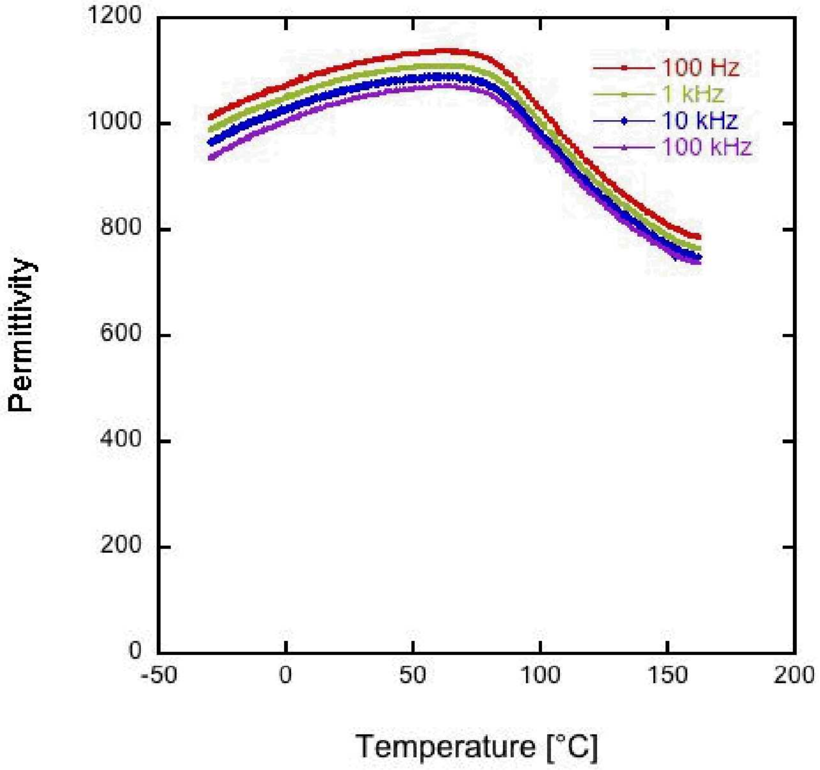

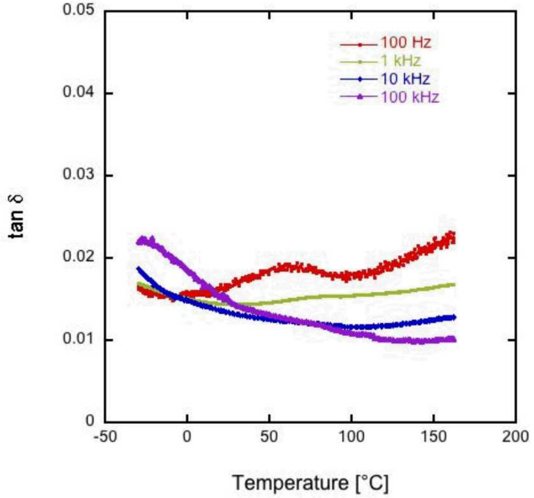

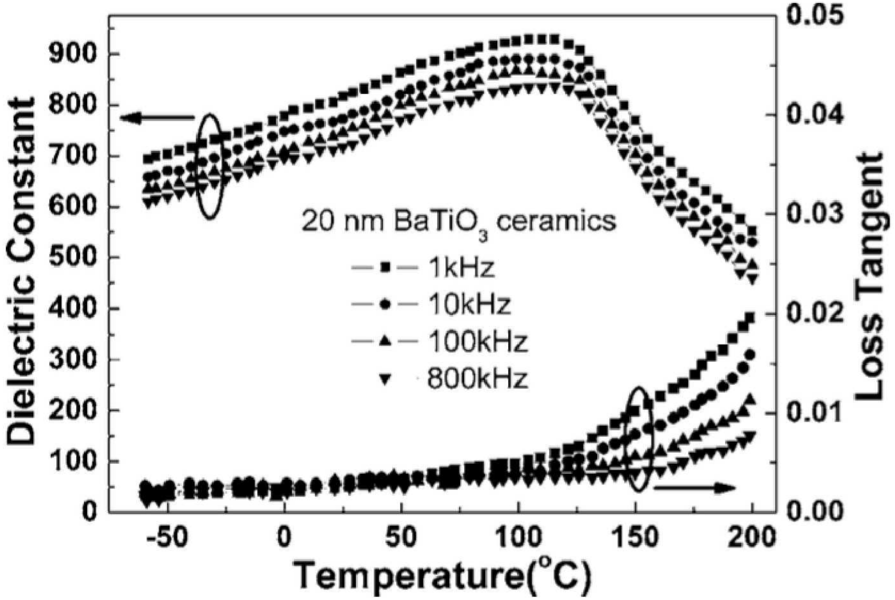

2006 Deng et al., *Appl. Phys. Lett*. **88**, 252905

- **SNL BTO, ~23 nm sample (no cracks, data on cooling)**
- **No obvious transition at Curie temp. (125 °C)**
- **Loss generally low but not consistent**
- **Data trend agrees with existing literature**

P vs. E

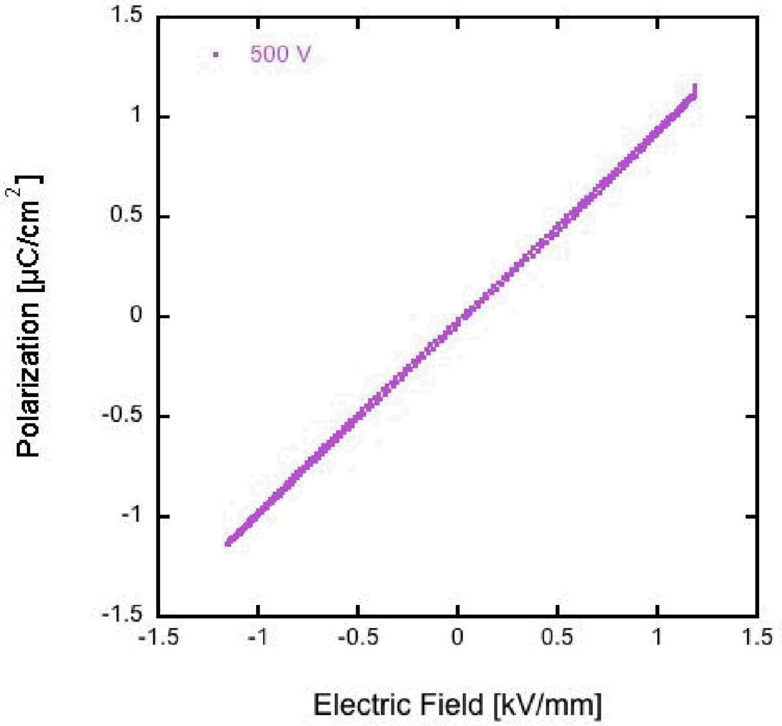

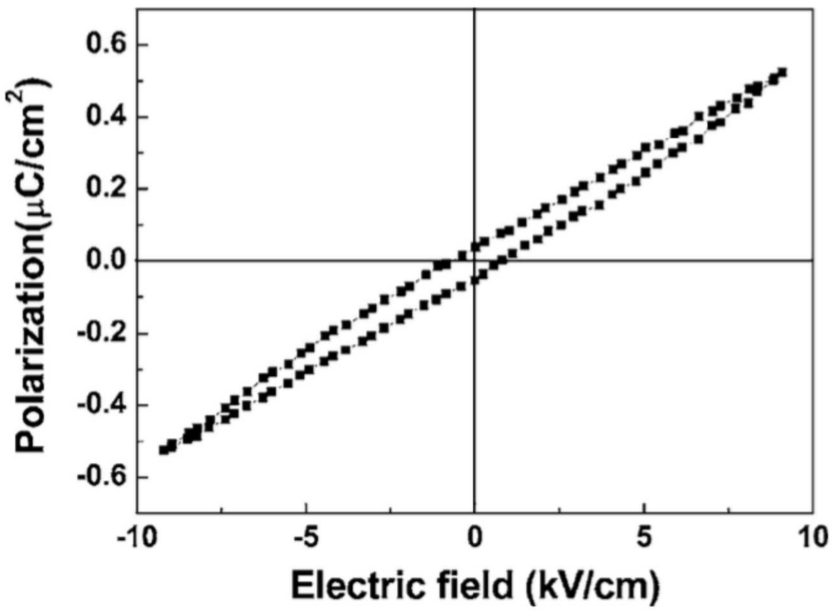

2006 Deng et al., *Appl. Phys. Lett*. **88**, 252905

- **SNL BTO at 100 Hz and NanOxide powder at 1 Hz**
- **Compares very favorably to work by Deng *et al.* from 2006**
- **Doubled polarization at equivalent fields**
- **Measured up to higher fields**
    - **Indicates likely a problem with breakdown in their sample**

U.S. NAVAL RESEARCH LABORATORY

P vs. E

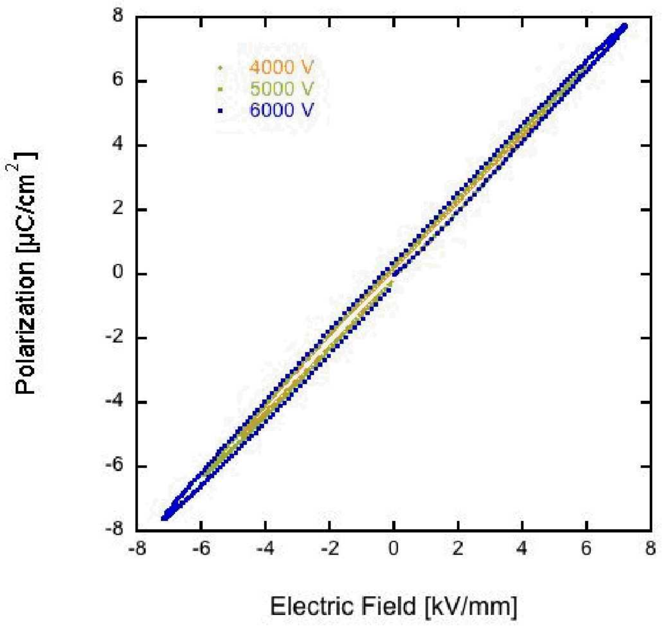

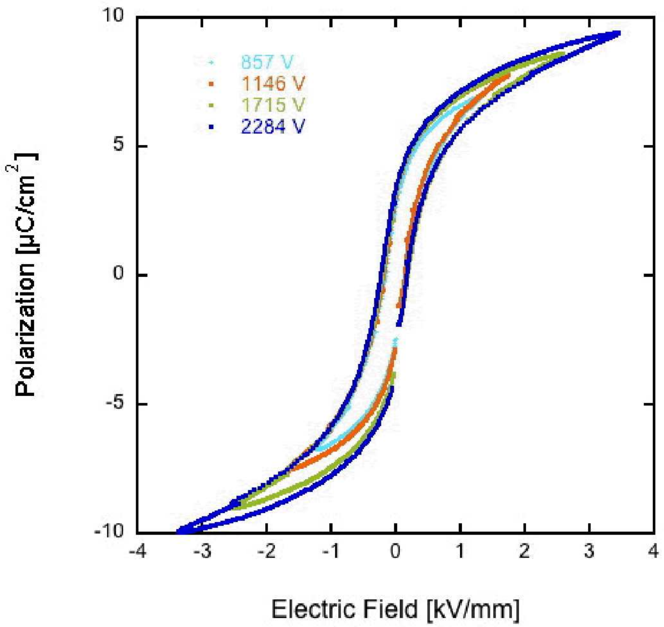

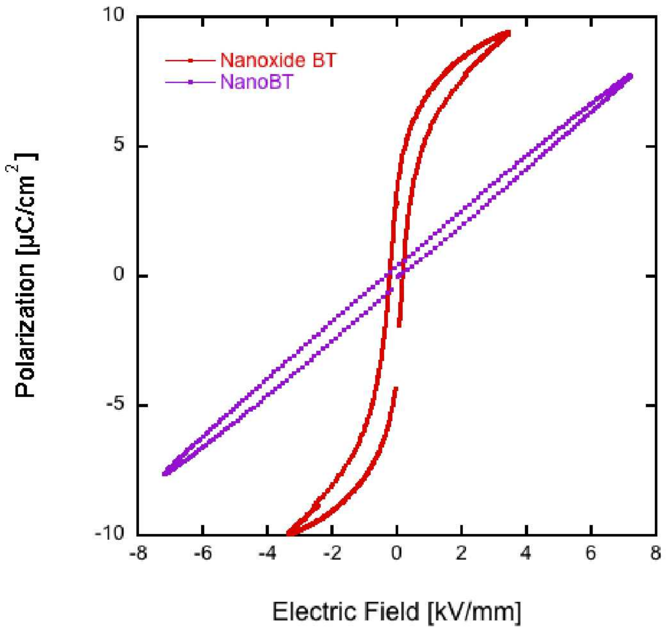

20.5 nm

Larger grain size
(Initial particle size 500nm)

SNL BTO at 100 Hz and NanOxide large grain ceramic at 1 Hz

U.S. NAVAL RESEARCH LABORATORY

Conclusions

- **SPS is a useful tool for consolidating dense, fine grain materials with excellent properties**
- **Tuning of desired response is possible through sintering parameters**
- **However, a high quality starting material cannot be overlooked!**

Acknowledgements

- We thank Robert Delaney (Univ. of NM) for his assistance with magnetic data analysis
- Harvey Mudd College: Albert Dato, Peter Saeta, Dick Haskell and many, many students
- Columbia University: Simon Billinge and Chenyang Shi
- NRL: Eric Patterson and Ed Gorzkowski
- UC Davis: Ricardo Castro and Martin Fraga
- We wish to thank Dr. Susan Heidger of the Air Force Research Laboratory/High Power Microwave Division for significant support of the work on ferroelectrics
- Magnetic material R&D supported by Dr. Imre Gyuk and the Energy Storage Program in the Office of Electricity Delivery and Energy Reliability at the US Department of Energy

AIR FORCE RESEARCH LABORATORY

U.S. NAVAL RESEARCH LABORATORY

Backup Slides

Benefits of a High Frequency Transformer

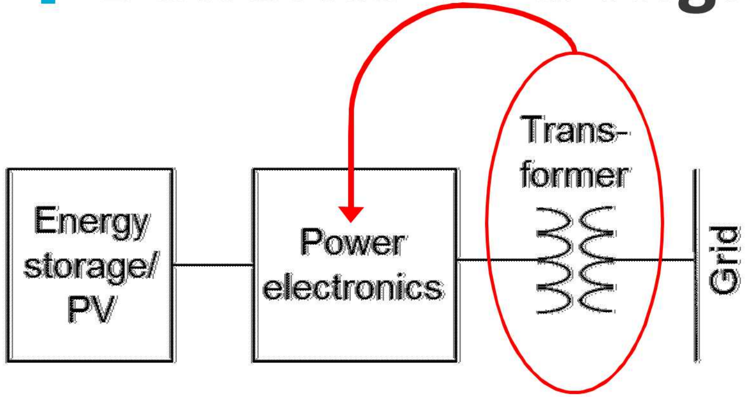

Line frequency (50 Hz) transformer

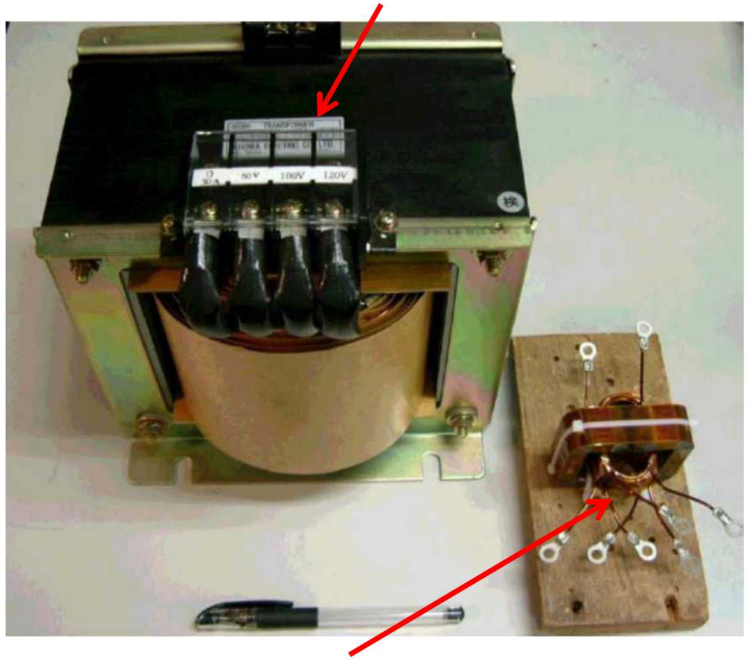

High frequency (20 kHz) transformer

S. Krishnamurthy, Half Bridge AC-AC Electronic Transformer, IEEE, 1414 (2012).

- **Integrate output transformer within power conversion electronics**
- **Leverage high switching speed, voltage, and temperature performance of WBG semiconductors**
- **Core materials for high frequency transformers have been an afterthought**

Material requirements:

- **Low loss over 10-200 kHz frequency range**
  - **low coercivity, high ρ**
- **High $J_s \rightarrow$ high power density**
- **High temperature performance**
- **Scalable & Affordable**
- **Increased reliability and better SWaP**

Magnetic Properties

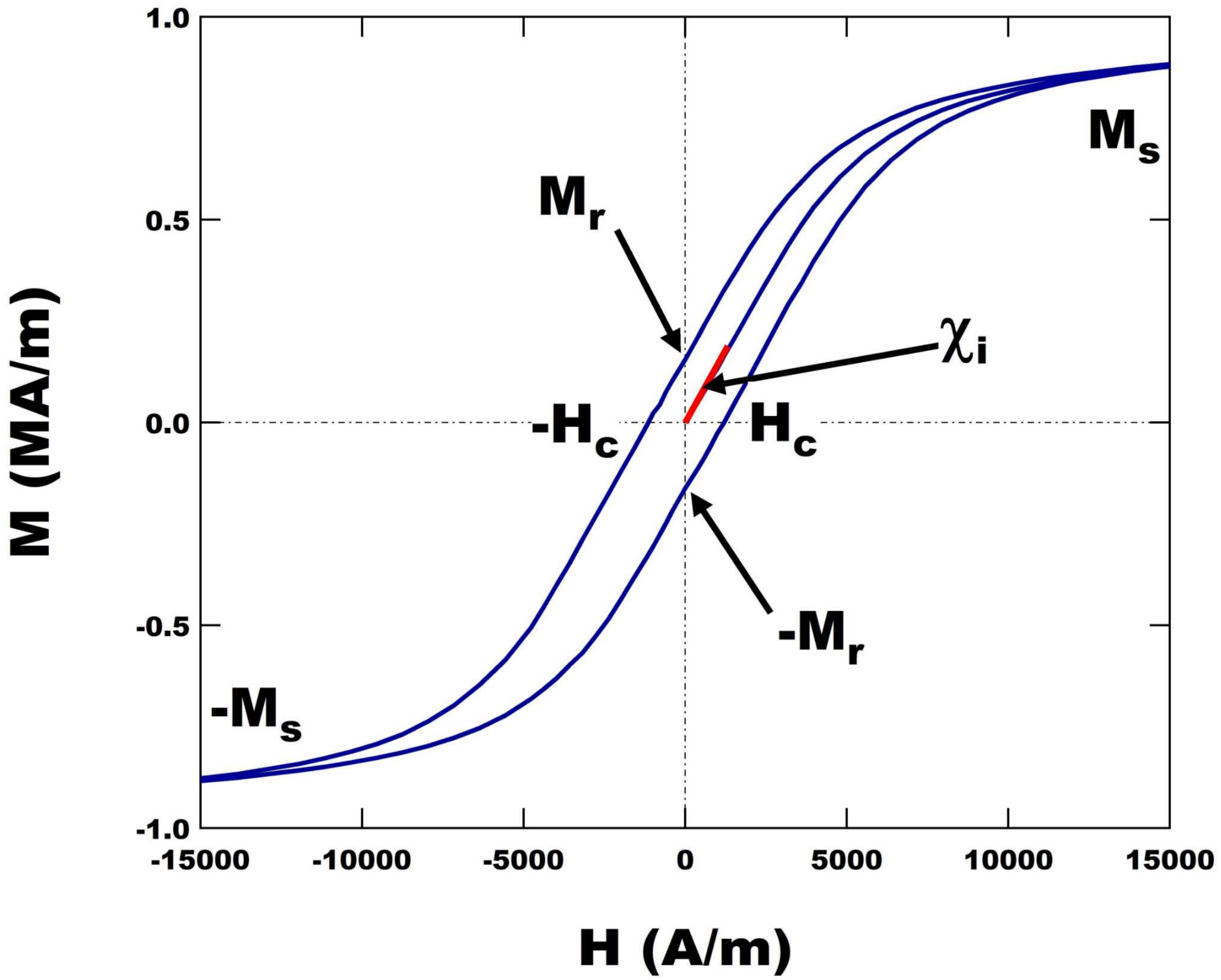

M_s = saturation magnetization

M_r = magnetic remnance

H_c = coercivity

χ_i = initial susceptibility

μ = permeability

μ_r = permeability

$\mu_r = \mu/\mu_0 = 1 + \chi$

Previous Syntheses of γ'-Fe_4N

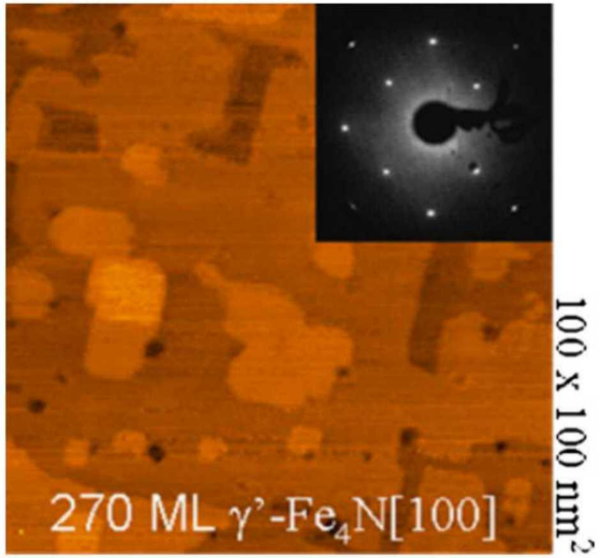

Fig. 1. STM image of a 270 monolayers (ML) thick γ'-Fe_4N film grown on Cu(1 0 0). The inset shows the corresponding LEED pattern (110 eV).

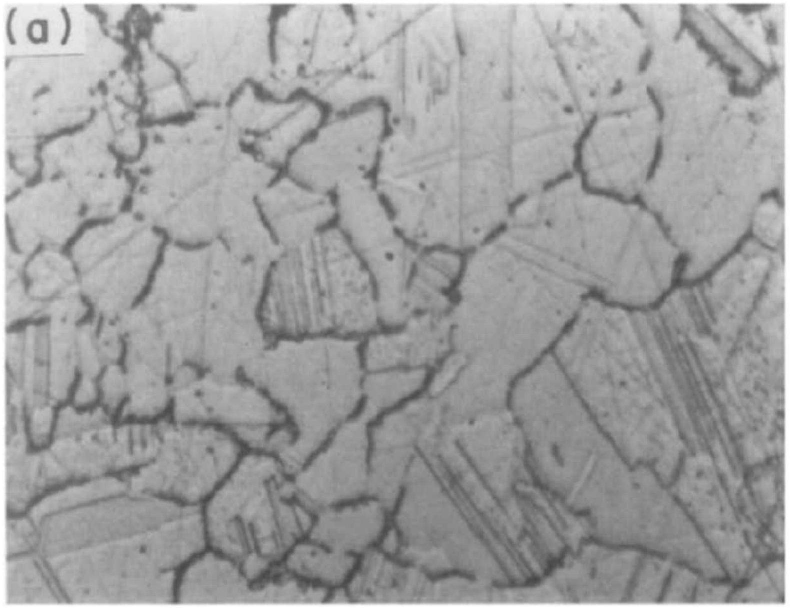

D. Ecija, et. al., "Magnetisation reversal of epitaxial films of γ'-Fe_4N on Cu(100)", J. Magn. Mag. Mat., 316, 321 (2007).

S.K. Chen, et. al., "Synthesis and magnetic properties of Fe_4N and $(Fe, Ni)_4N$ sheets", J. Magn. Mag. Mat., 110, 65 (1991).

Up to 50 nm thick

25 µm foils

$BaTiO_3$ (BTO) Nanoparticles Studied

Source	Name	Primary Particle Diameter (nm)	Synthesis Method
Sandia	SNL	10	80°C solution
Sakai	KZM-50	50	hydrothermal
Sakai	BT-01	100	hydrothermal
Sakai	BT-02	200	hydrothermal
Sakai	BT-03	300	hydrothermal
Sakai	BT-04	400	hydrothermal
Sakai	BT-05	500	hydrothermal

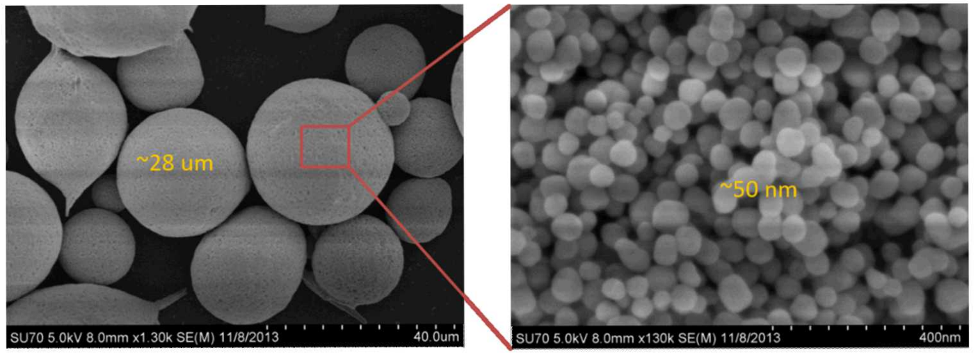

Sakai KZM-50

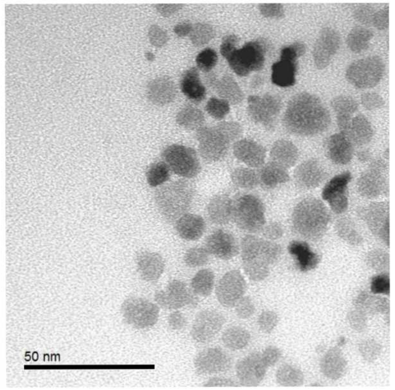

Sandia solution synthesized $BaTiO_3$

Ti Displacement

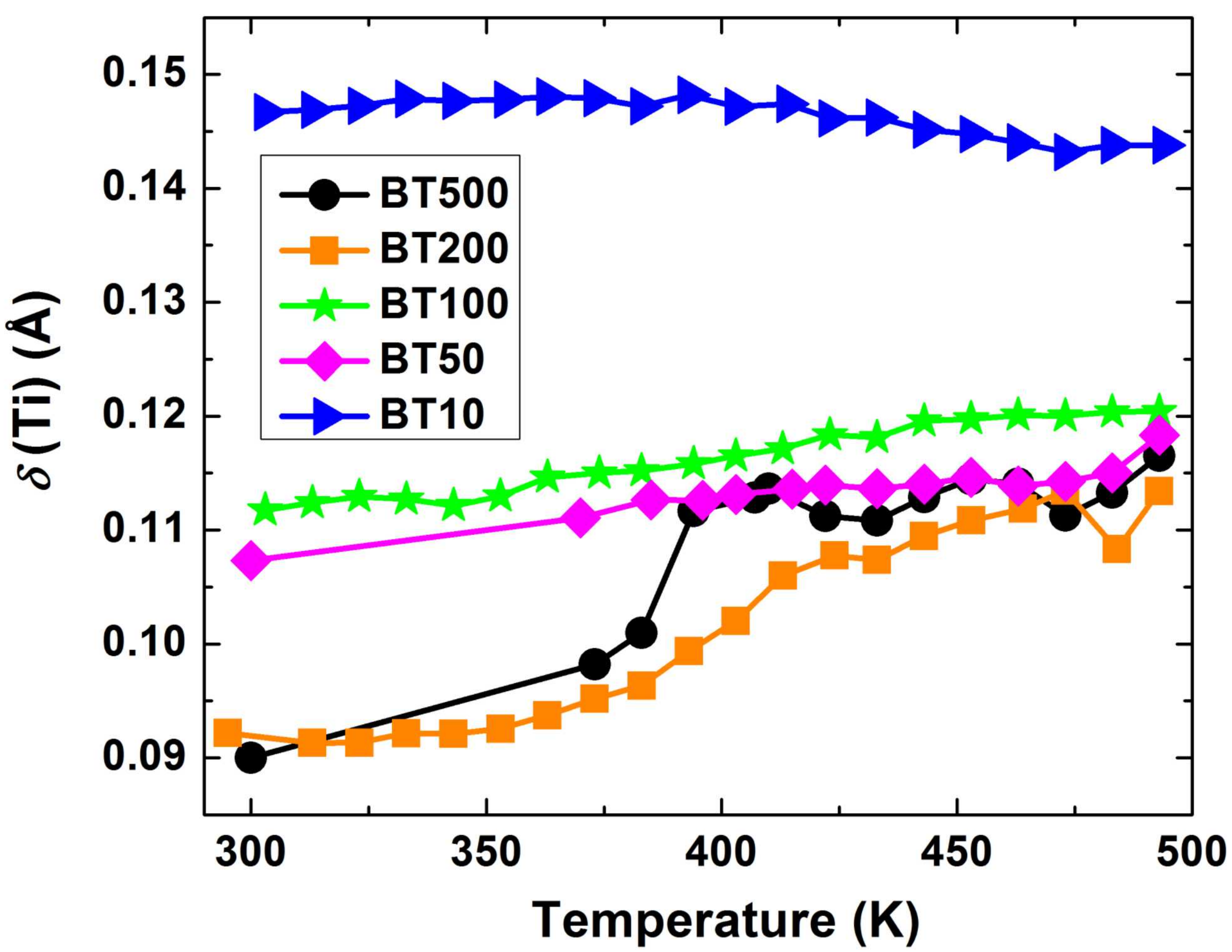

< 393.15 K

> 393.15 K

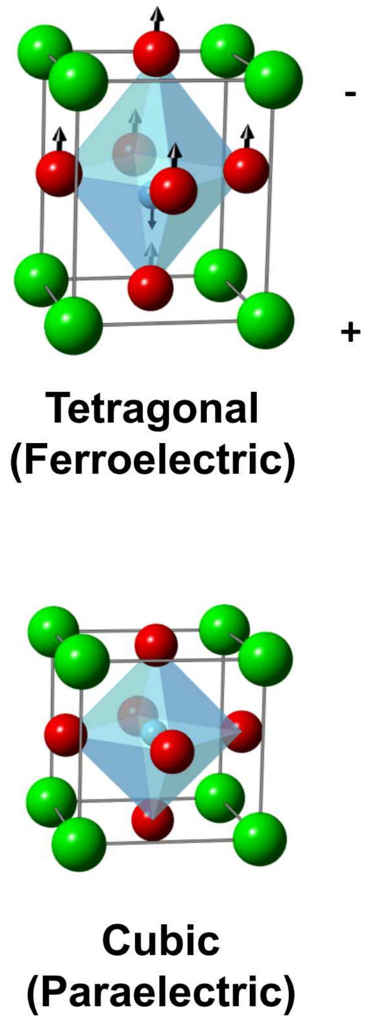

Synchrotron X-ray data collected at NSLS at Brookhaven National Lab

Size Dependent Behavior Observed with Raman

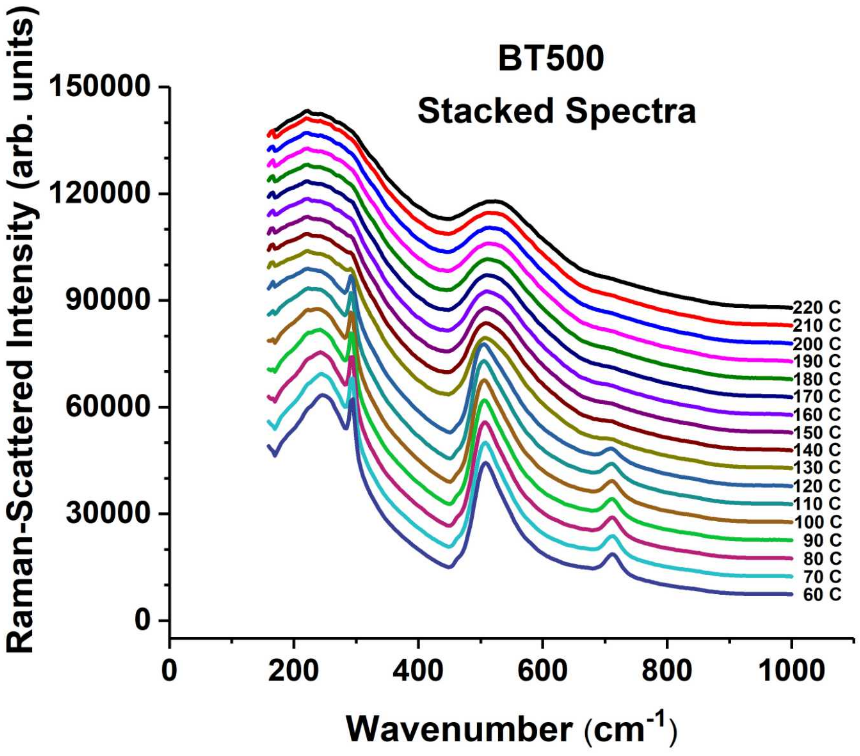

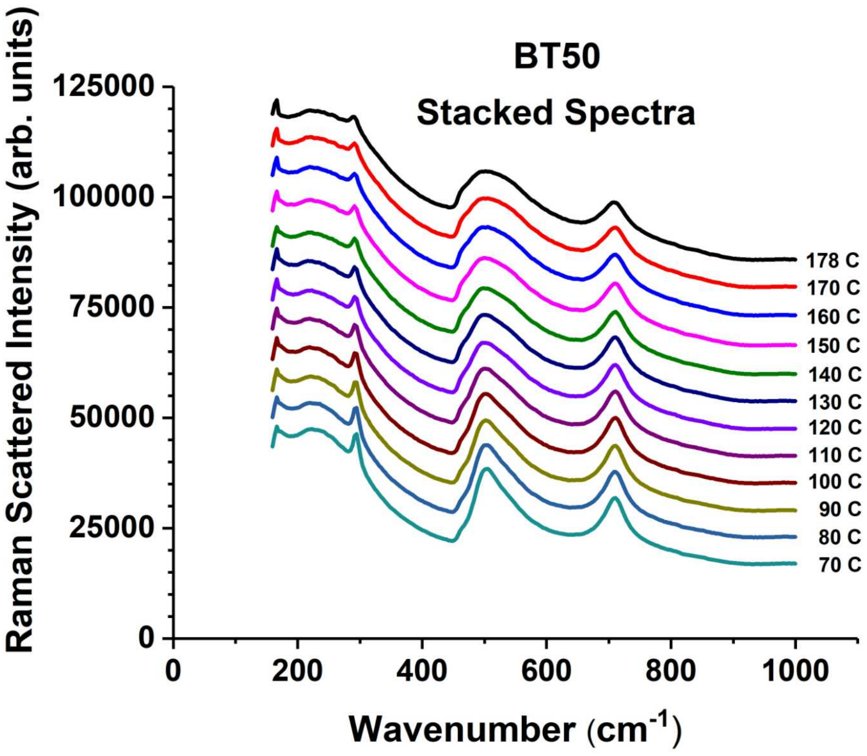

- **500 nm BTO: tetragonal Raman lines disappear abruptly at 120°C**
- **50 nm BTO: tetragonal Raman lines persist above 120°C**

HARVEY MUDD COLLEGE

Order Disorder Model

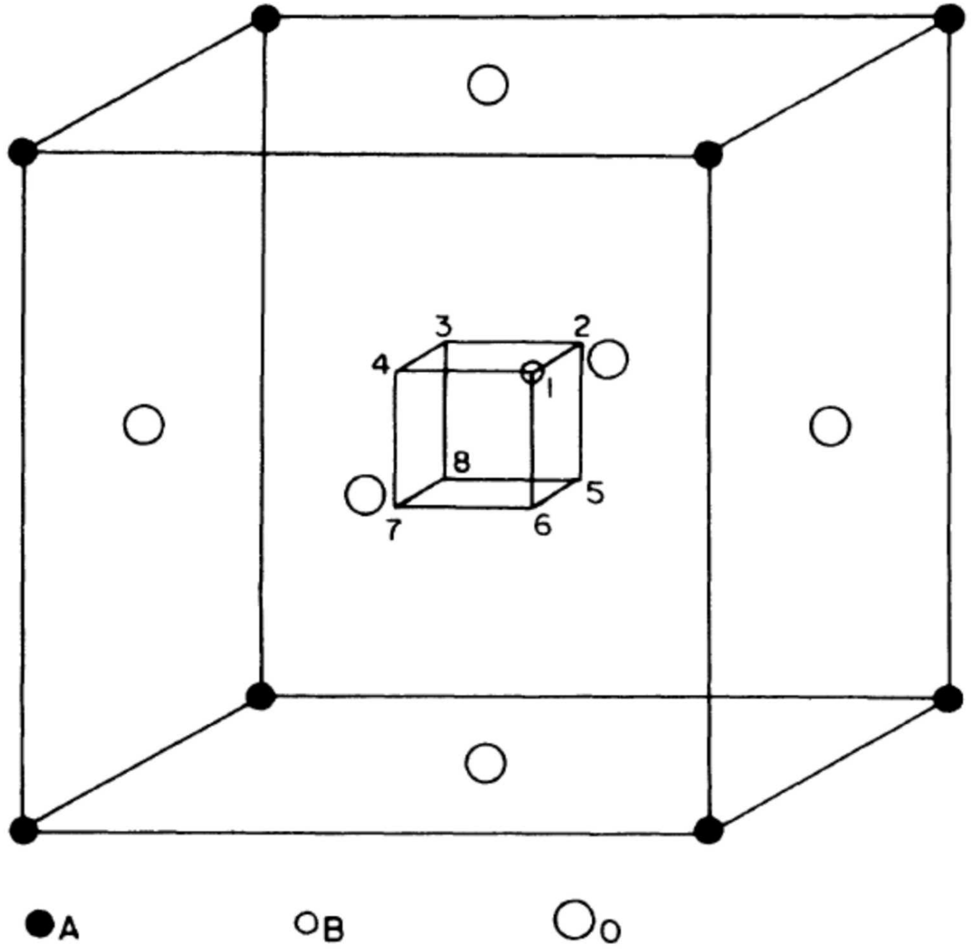

FIG. 1. Unit cell of the perovskites $BaTiO_3$ and $KNbO_3$ as proposed by Comes *et al.*

Chaves et. al., *Phys. Rev. B.* 13 207 (1976)